1 Phyllosphere exudates select for distinct microbiome members in sorghum epicuticular wax and
2 aerial root mucilage
3
4 Marco E. Mechan-Llontop[1,2], John Mullet[2,3], and Ashley Shade[1,2,4,5,6*]
5
6 [1]Department of Microbiology and Molecular Genetics, Michigan State University, East Lansing,
7 MI, 48824.
8 [2]Great Lakes Bioenergy Research Center, Michigan State University, East Lansing, MI, 48824.
9 [3]Department of Biochemistry & Biophysics, Texas A&M University, College Station, TX,
10 77843
11 [4]Department of Plant, Soil and Microbial Sciences, Michigan State University, East Lansing MI
12 48824
13 [5]The Plant Resilience Institute, Michigan State University, East Lansing MI 48824
14 [6] Univ Lyon, CNRS, INSA Lyon, Université Claude Bernard Lyon 1, École Centrale de Lyon,
15 Ampère, UMR5005, 69134, Ecully cedex, France. *(Present address)*
16
17 *Corresponding author: A. Shade; E-mail: ashley.shade@cnrs.fr
18
19 **ABSTRACT**
20
21 Phyllosphere exudates create specialized microhabitats that shape microbial community diversity.
22 We explored the microbiome associated with two sorghum phyllosphere exudates, the epicuticular
23 wax and aerial root mucilage. We assessed the microbiome associated with the wax from sorghum

plants over two growth stages, and the root mucilage additionally from nitrogen-fertilized and non-fertilized plants. In parallel, we isolated and characterized hundreds of bacteria from wax and mucilage, and integrated data from cultivation-independent and cultivation-dependent approaches to gain insights into exudate diversity and bacterial phenotypes. We found that *Sphingomonadaceae* and *Rhizobiaceae* families were the major taxa in the wax regardless of water availability and plant developmental stage to plants. The cultivation-independent mucilage-associated bacterial microbiome contained *Erwiniaceae, Flavobacteriaceae, Rhizobiaceae, Pseudomonadaceae, Sphingomonadaceae*, and its structure was strongly influenced by sorghum development but only modestly influenced by fertilization. In contrast, the fungal community structure of mucilage was strongly affected by the year of sampling but not by fertilization or plant developmental stage, suggesting a decoupling of fungal-bacterial dynamics in the mucilage. Our bacterial isolate collection from wax and mucilage had several isolates that matched 100% to detected amplicon sequence variants, and were enriched on media that selected for phenotypes including phosphate solubilization, putative diazotrophy, resistance to desiccation, capability to grow on methanol as a carbon source, and ability to grow in the presence of linalool and β-caryophyllene (terpenes in sorghum wax). This work expands our understanding of the microbiome of phyllosphere exudates and supports our long-term goal to translate microbiome research to support sorghum cultivation.

Keywords: bioenergy, agriculture microbiome, bacterial isolates, plant-association, diazotroph, irrigation, fertilizer, amplicon sequencing, cultivation

INTRODUCTION

47 The phyllosphere, which includes the above-ground plant structures, has diverse surface
48 features (Ruinen 1965; Vacher et al. 2016; Doan et al. 2020). It is a microbial habitat that is
49 exposed to rapid environmental fluctuations and stressors, including in ultraviolet radiation,
50 temperature, and nutrient and water availability. Thus, the diversity and functions of the
51 phyllosphere microbiome reflects this complex habitat (Lindow and Brandl 2003; Vorholt 2012;
52 Vacher et al. 2016). To adapt to abiotic stresses, plants produce a diversity of exudates on their
53 external surfaces (Chai and Schachtman 2022). The secreted exudates vary in composition and
54 structure, creating specialized phyllosphere microhabitats (Galloway et al. 2020). Exudates that
55 accumulate in the phyllosphere include epicuticular wax on stems and leaves (Kunst and
56 Samuels 2003), sugar-rich mucilage on aerial root structures (Bennett et al. 2020), floral
57 nectaries (Rering et al. 2018), and extrafloral nectaries in stems and leaves (Pierce 2019).
58 Because of their potential as locations of microbial engagement with the host, research has been
59 initiated to explore these microbial communities that reside on phyllosphere exudates.
60 Plants secrete epicuticular wax on leaves, leaf sheaths, and stems for prevention of water
61 loss under drought stress (Xue et al. 2017), reflection of solar radiation (Steinmüller and Tevini
62 1985), and pathogen protection (Serrano et al. 2014; Wang et al. 2020). Epicuticular waxes are
63 enriched in long-chain hydrocarbons. The major wax components include alkanes, alcohols,
64 esters, and fatty acids, as well as varying levels of triterpenoids, sterols, and flavonoids (von
65 Wettstein-Knowles 1974; Kunst and Samuels 2003; Busta et al. 2021). The wax composition and
66 quantities are affected by plant species, plant developmental stage, and environmental conditions
67 (Yeats and Rose 2013). It has been shown that epicuticular waxes affect bacterial and fungal
68 plant colonization in a species-dependent manner (Beattie and Marcell 2002; Tsuba et al. 2002).
69 Also, wax accumulation and composition directly impact the phyllosphere microbial community

70 diversity (Reisberg et al. 2013). A study in *Arabidopsis thaliana* reported that Proteobacteria,
71 Bacteroidetes, and Actinobacteria were the dominant phyla associated with wax on leaves
72 (Reisberg et al. 2013).

73 Plants also secrete an abundance of polysaccharide-rich mucilage on aerial roots and the
74 above ground portion of brace roots. Brace roots support plant anchorage as well as water and
75 nutrient uptake (Stamp and Kiel 1992; Ku et al. 2012; Reneau et al. 2020). In 2018, van Deynze
76 et al. 2018 reported that the mucilage of aerial roots of a maize landrace harbored diazotrophic
77 microbiota that provided almost 80% of the nitrogen needed by the host. The bacterial genera
78 *Acinetobacter*, *Agrobacterium*, *Enterobacter*, *Klebsiella*, *Lactococcus*, *Pantoea*, *Pseudomonas*,
79 *Rahnella*, *Raoultella*, *Stenotrophomonas*, and others have been found in association with the
80 mucilage of maize. These bacteria were capable of biological nitrogen fixation (BNF),
81 synthesizing indole-3-Acetic Acid (IAA), utilizing 1-amino-1-cyclopropanecarboxylic acid
82 (ACC), and solubilizing phosphates. The unique polysaccharide composition of the mucilage
83 may modulate its associated microbiota (van Deynze et al. 2018; Higdon et al. 2020b). The
84 maize mucilage is enriched in a mixture of monosaccharides including fucose (28%), galactose
85 (22%), arabinose (15%), glucuronic acid (11%), xylose (11%), mannose (8%), glucose (1%) and
86 galacturonic acid (1%) (van Deynze et al. 2018; Amicucci et al. 2019). The polysaccharide
87 composition of root mucilage may vary among maize genotypes and with changing
88 environmental conditions (Nazari et al. 2020).

89 Bioenergy sorghum (*Sorghum bicolor* L. Moench) is a heat and drought-tolerant annual
90 crop being developed for production of biomass, biofuels and bioproducts (Mullet et al. 2014;
91 Varoquaux et al. 2019). Bioenergy sorghum confers 75%-90% greenhouse gas mitigation when
92 used for ethanol production or biopower generation respectively (Olson et al. 2012), but excess

93 nitrogen fertilizer is required to grow it, resulting in the release of nitrous oxide and relatively
94 lower carbon benefit than other biofuel feedstocks that do not have high fertilizer demands (Kent
95 et al. 2020; Scully et al. 2021). In the 1980s, it was hypothesized that the mucilage secreted by
96 sorghum aerial roots harbors diazotroph bacteria, as has been more recently shown in the a maize
97 landrace (Bennett et al. 2020), but this has not yet been experimentally confirmed. Although the
98 polysaccharide composition of the sorghum aerial root mucilage is uncharacterized, it is
99 expected that the sorghum mucilage is similar in composition to maize (van Deynze et al. 2018;
100 Amicucci et al. 2019). Taken together, it is expected that understanding microbiome interactions
101 on the sorghum mucilage may provide insights into microbiome-enabled solutions to optimize
102 diazotrophic nitrogen for the host and, in parallel, reduce nitrogen fertilizer needs for bioenergy
103 sorghum.

104 Like other plants, bioenergy sorghum accumulates high levels of epicuticular wax on
105 stems and leaves over its development, and some functions of the wax are to exclude pathogens
106 and prevent water loss. Sorghum epicuticular wax chemistry and structure have been extensively
107 studied. The accumulation, and composition of sorghum epicuticular wax are affected by several
108 factors, including plant age, genotype, water availability, and environmental stresses (Bianchi et
109 al. 1978; Avato et al. 1984; Jordan et al. 1984; Steinmüller and Tevini 1985; Shepherd et al.
110 1995; Jenks et al. 1996; Bondada et al. 1996; Shepherd and Wynne Griffiths 2006; Xue et al.
111 2017). However, the influence of sorghum wax chemistry on bacteria colonization and
112 community structure is unknown.

113 In the present study, we investigated the microbiome associated with bioenergy sorghum
114 epicuticular wax and aerial root mucilage. Given the functions of these exudates for the host,
115 these communities may be of interest to examine microbiome traits that support host drought

116 tolerance and nutrient uptake. To begin to explore the microbial communities inhabiting these
117 specialized phyllosphere exudates, the microbiome composition and structure of wax and
118 mucilage was analyzed from field conditions that included management treatments expected to
119 influence plant water and nitrogen status. Specifically, we assessed the bacterial
120 microbiome associated with the epicuticular wax from sorghum plants at two different
121 developmental stages that also received different amounts of water, and the bacterial and fungal
122 microbiomes additionally associated with the aerial root mucilage from nitrogen (N)-fertilized
123 and non-fertilized sorghum plants. In addition, we curated a bacterial isolate collection from each
124 phyllosphere exudate. We integrate data from both cultivation-independent and -dependent
125 approaches to gain deeper insights into the microbiome diversity and dynamics of sorghum
126 epicuticular wax and aerial root mucilage.

127 We hypothesized that: 1) wax and mucilage harbor different bacterial microbiomes due to
128 their different exudate chemistries, host functions, and compartments; 2) plant developmental
129 stage and watering status has highest explanatory value for the wax bacterial microbiota due to
130 the known role of wax in supporting plant drought tolerance; 3) fertilization status has highest
131 explanatory value for the mucilage bacterial microbiota due to changes in exogenous nutrient
132 availability that are expected to result in changes in mucilage polysaccharide composition; and 4)
133 that the bacterial and fungal members of the mucilage microbiome exhibit similar dynamics due
134 to expected similar host and environmental drivers.

135

136 **METHODS**

137

138 **Collection of sorghum stems and recovery of epicuticular wax**. We collected samples from
139 the bioenergy sorghum *(Sorghum bicolor)* hybrid TX08001 grown at the Texas A&M University
140 Research Farm in College Station, Texas (30°55'5.55" N, 96°.43'64.6" W). Sorghum plants were
141 grown in 5 replicate 32 rows by 30 m plots at standard planting density and fertilization (Olson
142 et al., 2012). We sampled replicate plots 1-5 at 60 (08/03/2020) and 90 (09/02/2020) days after
143 plant emergence (DAE). While sorghum plants at 60 DAE were irrigated to maintain non-
144 limiting water status, plants at 90 DAE were grown without irrigation to induce water-limiting
145 conditions until harvesting. Thus, the developmental age of the plants and their watering status
146 are colinear and their effects cannot be separated in our study. We collected stem sections that
147 were covered in epicuticular wax, using razor blades to destructively sample the fifth and sixth
148 fully elongated stem node-internodes below the growing zone into sterile whirl-pak bags. In
149 total, we collected 50 stem samples during the growing season of 2020. All samples were kept on
150 ice for transport, shipped on dry ice to Michigan State University, and then stored at -80 °C. We
151 used sterile razor blades to carefully remove and collect the epicuticular wax from stems in
152 sterile 1.5 ml Eppendorf tubes. Epicuticular wax samples were stored at -80 °C until processing.
153
154 C**ollection of sorghum aerial roots and removal of the mucilage**. We collected samples from
155 the bioenergy sorghum cultivar TAM 17651 grown at the Great Lakes Bioenergy Research
156 Center (GLBRC), as part of the Biofuel Cropping System Experiment (BCSE) in Hickory
157 Corners, Michigan (42°23'41.6" N, 85°22'23.1" W). Sorghum plants were grown in 5 replicate
158 30x40 m plots arrayed in a randomized complete block design. Within each plot, nitrogen
159 fertilizer-free subplots were maintained either in the western or eastern -most 3m of each plot.
160 We sampled replicate plots 1-4 in both the main and nitrogen-fertilizer free subplots at 60 and 90

161 DAE. We used sterile razor blades to carefully collect between 3 to 5 aerial nodal roots per plant
162 that were covered with visible mucilage into sterile 50 ml Eppendorf tubes. In total, we collected
163 180 aerial root samples during the growing seasons of 2020 and 2021. All samples were kept on
164 ice for transport, and then stored at -80 ^{o}C. In the laboratory, we added 15 ml of sterile distilled
165 water and kept the roots for 5 min at room temperature to fully hydrate the aerial root mucilage.
166 We collected 1 ml of mucilage into sterile 1.5 ml Eppendorf tubes per sample. Mucilage samples
167 were stored at -80 ^{o}C until processing.
168
169 **Culturing the epicuticular wax and mucilage microbiomes.** For bacterial isolation, we pooled
170 the epicuticular wax collected from different plants, as described above, and resuspended 100 mg
171 of wax in 1 ml of sterile distilled water. We also pooled the mucilage collected from different
172 plants, as described above. To capture a diversity of bacteria from the wax and mucilage, we
173 used a variety of cultivation media (**Table 1**). First, we used standard culture media with a
174 relatively high concentration of nutrients, including Tryptic Soy Agar (TSA: casein peptone 15
175 gl^{-1}, soy peptone 5 gl^{-1}, sodium chloride 5 gl^{-1}, agar 15 gl^{-1}, pH 7.3) and 50TSA (1/2 dilution of
176 TSA). We also used media with relatively lower concentrations of nutrients, including
177 Reasoner's 2A (R2A: yeast extract 0.5 gl^{-1}, proteose peptone N°3 0.5 gl^{-1}, casamino acids 0.5 gl^{-}
178 ^{1}, glucose 0.5 gl^{-1}, soluble starch 0.5 gl^{-1}, sodium pyruvate 0.3 gl^{-1}, K_2HPO_4 0.3 gl^{-1}, $MgSO_4$ x
179 $7H_2O$ 0.05 gl^{-1}, agar 15 gl^{-1}), 50R2A (1/2 dilution of R2A), and M9 minimal media (Na_2HPO_4
180 12.8 gl^{-1}, KH_2PO_4 3.0 gl^{-1}, NaCl 0.5 gl^{-1}, NH_4Cl 1.0 gl^{-1}, glucose 20 gl^{-1}, 1M $MgSO_4$ solution 20
181 ml, 1M $CaCl_2$ solution 0.1 ml, thiamine 0.5% w/v solution 0.1 ml, agar 15 gl^{-1}). To enrich for
182 bacteria with putative plant beneficial traits, we used selective media types, including Jensen's
183 medium (sucrose 20 gl^{-1}, K_2HPO_4 1 gl^{-1}, $MgSO_4$ 0.5 gl^{-1}, NaCl 0.5 gl^{-1}, $FeSO_4$ 0.1 gl^{-1}, Na_2MoO_4

184 0.005 gl^{-1}, $CaCO_3$ 2 gl^{-1}, agar 1 gl^{-1}) and modified nitrogen-free M9 minimal media with and
185 without 1% (w/v) D-arabinose, galactose or xylose at pH 5, 5.8 or 7 (Na_2HPO_4 12.8 gl^{-1},
186 KH_2PO_4 3.0 gl^{-1}, NaCl 0.5 gl^{-1}, 1M $MgSO_4$ solution 20 ml, 1M $CaCl_2$ solution 0.1 ml, agar 15 gl^{-}
187 ^{1}) for detection of putative nitrogen fixing bacteria, Pirovskaya's agar (yeast extract 0.5 gl^{-1},
188 dextrose 10 gl^{-1}, $Ca_3(PO_4)_2$ 5 gl^{-1}, $(NH_4)_2SO_4$ 0.5 gl^{-1}, KCl 0.2 gl^{-1}, $MgSO_4$ 0.1 gl^{-1}, $MnSO_4$
189 0.0001 gl^{-1}, $FeSO_4$ 0.0001 gl^{-1}, agar 15 gl^{-1}) for detection of phosphate solubilizing bacteria,
190 Gauze's synthetic medium N°1 (soluble starch 20 gl^{-1}, KNO_3 1 gl^{-1}, NaCl 0.5 gl^{-1}, $MgSO_4$ x
191 $7H_2O$ 0.5 gl^{-1}, K_2HPO_4 0.5 gl^{-1}, $FeSO_4$ x 7 H_2O 10 mgl^{-1}, agar 15 gl^{-1}) for isolation of
192 Actinobacteria, King's medium B (proteose peptone 20 gl^{-1}, K_2HPO_4 1.5 gl^{-1}, $MgSO_4$ x $7H_2O$ 1.5
193 gl^{-1}, glycerol 10 ml) for isolation of fluorescent pseudomonas, and methanol mineral salts
194 medium ($(NH_4)_2SO_4$ 2.0 gl^{-1}, NH_4Cl 2.0 gl^{-1}, $(NH_4)_2HPO_4$ 2.0 gl^{-1}, KH_2PO_4 1.0 gl^{-1}, K_2HPO_4 1.0
195 gl^{-1}, $MgSO_4$ x $7H_2O$ 0.5 gl^{-1}, Fe_2SO_4 x $7H_2O$ 0.01 gl^{-1} ,$CaCl_2$ x $2H_2O$ 0.01 gl^{-1}, yeast extract 2.0
196 gl^{-1}, agar 20 gl^{-1}) for isolation of methanol-utilizing bacteria.

197 All plates were incubated for up to 14 days. To select for anaerobic bacteria, agar plates
198 were placed in anaerobic jars (Mitsubishi AnaeroPack 7.0L rectangular jar) containing three bags
199 of anaerobic gas generator (Thermo Scientific AnaeroPack Anaerobic Gas generator). To enrich
200 for bacteria resistant to desiccation, one hundred microliters of dilution 10^{-1} from the wax and
201 mucilage were inoculated on 20 ml of 50% TSB liquid culture supplemented with different
202 concentrations of 6000 polyethylene-glycol, including –0.49 MPa (210 gl^{-1} PEG w/v), -0.73 MPa
203 (260 gl^{-1} PEG w/v) and –1.2 MPa (326 gl^{-1} PEG w/v). To enrich for bacteria that can grow in the
204 presence of terpenoids, 100 ml of dilution 10^{-1} from the wax and mucilage were inoculated on 20
205 ml of 50% TSB liquid culture supplemented with 1% (v/v) of either linalool or β-caryophyllene.
206 Liquid cultures were incubated at 28°C for 24 h, and dilutions 10^{-1} to 10^{-4} were plated in

207 duplicate on R2A agar plates for 24 h. Well isolated individual colonies were picked with a
208 sterile toothpick and transferred to a new R2A plate. To confirm bacterial purity, individual
209 bacterial colonies were transferred three times on new R2A agar plates. Glycerol stock (25% v/v)
210 of pure bacteria isolates were stored at -80°C.
211
212 **Metagenomic DNA extraction and amplicon sequencing.** Microbial DNA was extracted from
213 0.5 ml of mucilage and 100 mg of epicuticular wax using a DNeasy PowerSoil kit (Qiagen,
214 Maryland, USA) according to the manufacturer's instructions. To confirm successful DNA
215 extraction, the metagenomic DNA was quantified using a qubit 2.0 fluorometer (Invitrogen,
216 Carlsbad, CA, USA), and visualized in a 1% agarose gel. Then, the PCR amplifications and
217 sequencing of the V4 region of the 16S rRNA bacterial or archaeal gene from the epicuticular
218 wax and mucilage samples and the ITS1 region of the fungal rRNA gene from the mucilage
219 samples only were performed. DNA concentrations were normalized to approximately 1 µg/µl
220 between all samples before PCR amplification and sequencing. The V4 hypervariable region of
221 the 16S rRNA gene was amplified using the universal primers 515F (5′-
222 GTGCCAGCMGCCGCGGTAA- 3′) and 806R (5′-GGACTACHVGGGTWTCTAAT-3′)
223 (Caporaso et al. 2011) under the following conditions: 95°C for 3 min, followed by 30 cycles of
224 95°C for 45 s, 50°C for 60 s, and 72°C for 90 s, with a final extension at 72°C for 10 min. The
225 metagenomic DNA of each sample was submitted to the Genomics Core of the Research
226 Technology Support Facility at Michigan State University for library preparation and sequencing
227 using the Illumina MiSeq platform v2 Standard flow cell in a 2x250bp paired-end format, using
228 their standard operating protocol.
229

230 The ITS1 region was amplified using primers ITS1f (5′-CTTGGTCATTTAGAGGAAGTAA-3′)
231 and ITS2 (5′-GCTGCGTTCTTCATCGATGC-3′) (Smith and Peay 2014) with the addition of
232 index adapters CS1-TS-F: 5' – ACACTGACGACATGGTTCTACA – [TS-For] – 3' and
233 CS2-TS-R: 5' – TACGGTAGCAGAGACTTGGTCT – [TS-Rev] – 3' as requested by the
234 Genomics Sequencing Core under the following PCR conditions: 94°C for 3 min, followed by 35
235 cycles of 94°C for 30 s, 52°C for 30 s, and 68°C for 30 s, with a final extension at 68°C for 10
236 min. The amplification was performed with GoTaq Green Master Mix (Promega). The PCR
237 products were purified with ExoSAP-IT reagent, and sample sequencing was completed by the
238 Genomics Core of the Research Technology Support Facility at Michigan State University using
239 the Illumina MiSeq platform v2 Standard flow cell in a 2x250bp paired-end format. For quality
240 control purposes, positive and negative controls were included throughout the DNA extraction,
241 PCR amplification, and sequencing processes. A 75 µl aliquot of the ZymoBIOMICS Microbial
242 Community Standard (Zymo Research, Irvine, CA, U.S.A) and 75 µl aliquot of an in-house
243 Community Standard were included as positive controls. Sterile DEPC-treated water was
244 included as negative control.
245
246 **Bacterial genomic DNA extraction.** Bacteria colonies that were first streaked and isolated for
247 purity were grown on 2 ml of 50% TSB liquid culture at 28°C for 24 h. Bacteria culture was
248 centrifuged at 5,000 rpm for 10 min. Genomic DNA of each isolate was extracted by using the
249 Zymo – Quick DNA Fungal/Bacterial 96 kit following the manufacturer's protocol. Total
250 genomic DNA was quantified using a qubit 2.0 fluorometer and visualized in a 1% agarose gel.
251 The PCR amplification of the full-length 16S rRNA gene with universal primers 27F (5′-
252 AGAGTTTGATCCTGGCTCAG-3′) and 1492R (5′-TACGGTTACCTTGTTACGACTT-3′)

253 (Miller et al. 2013) was performed by using the Pfu Turbo DNA polymerase (Agilent) under the
254 following conditions: 95°C for 2 min, followed by 24 cycles of 95°C for 30 s, 48°C for 30 s, and
255 72°C for 3 min, with a final extension at 72°C for 10 min. PCR products were purified with
256 ExoSAP-IT reagent and submitted for Sanger sequencing at the Genomics Core of the Research
257 Technology Support Facility at Michigan State University, MI, USA.
258
259 **Bacterial and fungal amplicon sequencing analysis**. Paired-end sequencing data from each
260 sequencing experiment were processed with QIIME2 (Bolyen et al. 2019) version 2021.8.0. In
261 brief, sequences were imported using the PairedEndFastqManifestPhred33V2 format. Sequence
262 quality control, denoising, and generation of feature tables containing counts for the Amplicon
263 Sequencing Variants (ASVs) were performed with the q2-dada2 plugin version 2021.8.0
264 (Callahan et al. 2016). Trimming parameters for the DADA2 plugin were selected with FIGARO
265 version 1.1.2 (Weinstein et al. 2019). ASVs tables and representative sequences from each
266 sequencing experiment were merged with the q2-feature-table plugin. ASV taxonomy (of
267 merged ASVs) was assigned with the q2-feature-classifier plugin using the SILVA version 1.38
268 database (Quast et al. 2013) for bacteria and UNITE version 8.3 database (Nilsson et al. 2019)
269 for fungi.
270 The ASV table, taxonomy table, and sample metadata files were imported into R version
271 4.1.3 for data visualization and statistical analysis. Diversity and statistical analyses were
272 performed using the phyloseq (McMurdie and Holmes 2013) and vegan (Dixon 2003) packages.
273 Treatments compared were: exudate (wax, mucilage) for bacterial microbiomes; fertilization
274 status (fertilized, unfertilized), year of sample collection (2020, 2021), and developmental stage
275 (60 DAE, 90 DAE) for mucilage bacterial and fungal microbiomes; and developmental

276 stage/water availability (60 DAE, 90 DAE) for wax bacterial microbiomes. A Wilcoxon rank
277 sum test with continuity correction was used to test for differences in alpha diversity across
278 treatments. Permuted analysis of variance (PERMANOVA) and permuted analysis of beta-
279 dispersion (PERMDISP) were used to assess differences in beta diversity structure across
280 treatments by centroid and dispersion. Differential abundance analysis was performed with the
281 DESeq2 package (Love et al. 2014). Each dataset (bacterial/fungal, wax/mucilage) was
282 subsampled independently to ensure maximum coverage for comparisons over time and across
283 field treatments. The exception was when testing hypothesis 1 (differences in wax and mucilage
284 bacterial microbiome), and in this case both datasets were subsampled to an even 2,500
285 sequences per sample for comparison.
286
287 **Full-length 16S rRNA gene Sanger sequencing analysis: Culturing phyllosphere exudate**
288 **microbiota.** To generate a consensus sequence of the full-length 16S rRNA gene from each
289 bacterial isolate, sequences were imported into Geneious version 2021.2.2
290 (https://www.geneious.com/). High-quality forward and reverse sequences were aligned and
291 trimmed to generate a consensus sequence. Then, the consensus sequence was searched with
292 BLAST for taxonomic classification. CD-HIT version 4.8.1 (Li and Godzik 2006) was used to
293 remove redundant 16S rRNA sequences. To identify bacterial isolates that match 100% to the
294 identified ASVs from the culture-independent approach, a local BLAST search was performed.
295 In summary, a local BLAST database was created with all non-redundant 16S rRNA sequences
296 from our bacterial collection using the *makeblastdb* command and the *-dbtype nucl* option. A
297 BLAST search was carried out to identify related sequences in the representative sequences
298 (ASVs dna-sequences.fasta) file generated from the DADA2 denoising step with the *blastn*

299 command, and the flowing options: "6 qseqid sseqid pident length mismatch gapopen qstart qend
300 sstart send evalue bitscore".
301
302 **Comparison with publicly available plant-associated bacterial genomes.** We retrieved 637
303 plant-associated (PA) bacterial genomes that were classified as non-root associated from the
304 (Levy et al. 2017) study. High-quality bacterial genomes were annotated with Prokka (Seemann
305 2014) using an in-house python script and annotated 16S rRNA gene copies were identified
306 (available on GituHub, see Data availability statement). For bacteria with multiple 16S rRNA
307 copies, CD-HIT version 4.8.1 (Li and Godzik 2006) was used to remove redundant sequences
308 (99% similarity) and one 16S rRNA sequence was conserved, totaling 433 unique PA sequences.
309 All 16S rRNA sequences from the PA bacterial genome dataset were concatenated in a single
310 fasta file with the *cat* command. CD-HIT was used to remove redundant sequences (100 %
311 similarity) from the 16S rRNA concatenated file. All non-redundant 16S rRNA sequences from
312 both the sorghum bacterial collections and the publicly available PA bacteria were merged in a
313 single *fasta* file. Sequence alignment was performed with MAFFT v7.407 (Katoh et al. 2002).
314 Alignment trimming was performed with trimAl (Capella-Gutiérrez et al. 2009). A maximum-
315 likelihood (ML)-based phylogenetic tree was built with IQ-TREE 2.2.0-beta version (Minh et al.
316 2020). ModelFinder version (-m TEST option) (Kalyaanamoorthy et al. 2017) was used to select
317 the best model for the phylogenetic tree construction. Branch support was assessed using 1,000
318 ultrafast boostrap approximations (-bb 1000 option) (Hoang et al. 2018). Phylogenetic diversities
319 were calculated as the total tree length, that represents the expected number of substitutions per
320 site. Phylogenetic tree was edited with iTOLs version 6.5.8 (Letunic and Bork 2021).
321

322 **Data and code availability.** The data analysis workflows for sequence processing and
323 ecological statistics are available on GitHub
324 (https://github.com/ShadeLab/Sorghum_phyllosphere_microbiome_MechanLlontop_2022.git).
325 Raw sequencing data has been deposited in the Sequence Read Archive NCBI database under
326 BioProject accession number PRJNA844896 (including 16S rRNA and ITS amplicons). Full-
327 length 16S rRNA sequence data has been deposited in the GenBank with accession numbers
328 ON973084-ON973283.
329
330 **RESULTS**
331 **Sequencing summary.** In total, we sequenced the bacterial 16S rRNA V4 region from 48
332 epicuticular wax samples from the 2020 growing season, as well as the bacterial 16S rRNA V4
333 region from 179 mucilage samples and the fungal ITS region from 173 mucilage samples that
334 were collected across two growing seasons in 2020 and 2021. We obtained 8,648,839 bacterial
335 sequences from the wax, and 20,606,039 bacterial and 20,181,404 fungal sequences from the
336 mucilage. After quality control, removal of chimeras, and denoising, 7,930,768 quality bacterial
337 reads were obtained from the wax samples, and 19,880,634 bacterial and 12,157,819 fungal
338 sequences were obtained from mucilage **(Table 2)**. For wax, the total number of sequences per
339 sample after the denoising process with DADA2 into Amplicon Sequence Variants (ASVs)
340 ranged from 1,722 to 272,108. After the removal of nonbacterial and unassigned sequences, a
341 total of 2,386,033 sequences remained, with sequencing reads per wax sample ranging from 138
342 to 206,128. We removed wax samples with fewer than 1000 sequences, and the remaining 42
343 epicuticular wax samples were rarefied to 1,303 sequences for further analysis **(Figure 1A)**.
344 Given the observed richness (12 to 93 ASVs per sample) by these cultivation-independent

345 methods, Figure 1A shows that the wax bacterial microbiome was covered with the given
346 sequencing effort.

347 For root mucilage, the number of bacterial sequences per sample after the denoising
348 ranged from 222 to 330,853. After the removal of nonbacterial and unassigned sequences, a total
349 of 12,956,774 sequences remained, with sequencing reads per sample ranging from 110 to
350 235,069. We removed samples with fewer than 20,000 sequences, and the remaining 158
351 samples were rarefied to 20,519 sequences for comparative analysis **(Figure 1B)**. Given the
352 observed richness (49 to 555 ASVs per sample) by these cultivation-independent methods,
353 Figure 1B shows that the mucilage bacterial microbiome was covered with the given sequencing
354 effort. The number of fungal sequences per mucilage sample after the denoising ranged from 78
355 to 119,207. After the removal of non-fungal and unassigned sequences, a total of 12,297,453
356 sequences remained, with sequencing reads per sample ranging from 32 to 119,207. We filtered
357 mucilage samples with fewer than 30,000 ITS sequences, and the remaining 171 samples were
358 rarefied to 33,975 sequences for comparative analysis **(Figure 1C)**. Similarly, given the
359 observed richness by these cultivation-independent methods (47 to 237 ASVs per sample),
360 **Figure 1C** shows that the mucilage fungal microbiome was covered with the given sequencing
361 effort.

362

363 **Hypothesis 1: Wax and mucilage harbor different bacterial microbiomes**

364 Compositional differences in the bacterial microbiomes of the epicuticular wax and mucilage
365 were apparent at the family level of taxonomic resolution (**Figure 2A and B)** as well as at the
366 genus level **(Supplementary Figure S1A and B**). Wax and mucilage bacterial microbiomes had
367 different richness (observed taxa Wilcoxon rank $p<0.001$, **Supplementary Table 1**) and

368 different structures (PERMANOVA R-squared= 0.14, *p*=0.001). Thus, Hypothesis 1 was
369 supported. However, there were no differences detected in the dispersions of wax and mucilage
370 bacterial microbiome structures (PERMDISP F=0.69, *p*=0.43).
371
372 **Hypothesis 2: Plant developmental stage/watering status has highest explanatory value for**
373 **the wax bacterial microbiota**
374 Altogether, we identified 534 bacterial ASVs in epicuticular wax. Wax bacterial microbiome
375 samples collected from sorghum plants at 60 DAE and 90 DAE had different richness (observed
376 taxa Wilcoxon rank *p*= 0.03) **(Supplementary Table 1)**. There was higher variation in the
377 community structure in the epicuticular wax on plants at 90 DAE compared with plants at 60
378 DAE (PERMDISP F=17.92, *p*=0.001). There was a small but significant influence of sorghum
379 developmental stage on the epicuticular wax community structure **(**PERMANOVA R-
380 squared=0.06, *p*= 0.003, **Figure 3A**, **Table 3)**.
381 The sorghum epicuticular wax microbiome was dominated by the Proteobacteria (84%
382 mean relative abundance) and Bacteroidetes (11%) bacteria phyla. The bacterial classes
383 Alphaproteobacteria (54%), Gammaproteobacteria (30%), and Bacteroidia (11%) were in highest
384 abundance. Sphingomonadaceae (25%), Rhizobiaceae (21%), and Xanthomonadaceae (7%) were
385 the major bacterial families in sorghum epicuticular wax **(Figure 2A).** At the genus level,
386 *Sphingomonas* (28%), *Rhizobium* (12%), *Aureimonas* (10%), and *Acinetobacter* (5%) were the
387 dominant taxa in wax **(Supplementary Figure 1)**. Differential abundance analysis showed that
388 only one ASV (ASV ID #5438e75153393c2dda98fe3d99c26da1) from the Microbacteriacea
389 family was more abundant on the wax of plants at 60 DAE (by 3.08-fold, DeSeq *p* = 0.01), and
390 that one ASV (ASV ID #8f820a46cfecd19477f4485d1c436764) assigned to *Pseudoxanthomonas*

391 genera was more abundant on the wax of plants at 90 DAE (by 4.49-fold, DESeq $p = 0.01$).
392 Taking these results together, Hypothesis 2 was weakly supported with a small, significant
393 difference in wax bacterial microbiome by plant stage and two taxa that were distinguishing
394 between the stages.
395

396 **Hypothesis 3: Fertilization status has highest explanatory value for the bacterial mucilage**
397 **microbiota**

398 Altogether, 12,047 bacterial ASVs were identified in aerial root mucilage. There was no
399 difference in richness between mucilage samples collected from sorghum plants at 60 DAE and
400 90 DAE (observed species Wilcoxon rank $p = 0.82$, **Supplementary Table 1**), and also no
401 difference between mucilage samples from nitrogen-fertilized plants as compared with
402 unfertilized plants. **(**observed species Wilcoxon rank $p = 0.15$, **Supplementary Table 1)**. There
403 was different beta dispersion in community structure by plant developmental stage (PERMDISP
404 F=19.56, p=0.001) but not by fertilization status (PERMDISP F=1.83, p=0.187). The mucilage
405 bacterial microbiome structure was better explained by developmental stage than fertilization
406 status (PERMANOVA R-squared= 0.14 and 0.03, respectively, both p= 0.001) **(Figure 3B).**
407 The aerial root mucilage bacterial microbiome was dominated by the Proteobacteria
408 (61% mean relative abundance) and Bacteroidota (36%) bacteria phyla. The bacterial class
409 Gammaproteobacteria (40%), Bacteroidia (34%), and Alphaproteobacterial (21%) were the most
410 abundant. Erwiniaceae (23%), Rhizobiaceae (14%), Flavobacteriaceae (12%),
411 Pseudomonadaceae (9%), and Sphingomonadaceae (6%) were the major bacterial families in
412 mucilage (**Figure 2B)**. A differential abundance analysis identified 25 ASVs enriched in the
413 mucilage at 60 DAE and 72 ASVs significantly enriched in plants at 90 DAE **(Figure 4,** DESeq

414 $p = 0.01$). Taking these results together, Hypothesis 3 was not supported, and the bacterial
415 microbiome of the mucilage was not highly sensitive in structure or dispersion to fertilization
416 given this study's field conditions, nor were there notable distinguishing taxa by plant
417 fertilization status.
418
419 **Hypothesis 4: The bacterial and fungal members of the mucilage microbiome exhibit**
420 **similar dynamics.**
421 Altogether, 5,641 fungal ASVs were identified in aerial root mucilage. There were differences in
422 richness between mucilage samples collected from sorghum plants during the 2020 and 2021
423 growing seasons (observed species Wilcoxon rank $p = 0.008$), and also between mucilage
424 samples from nitrogen-fertilized plants compared with unfertilized plants (observed species
425 Wilcoxon rank $p < 0.01$). However, no difference was observed between mucilage samples from
426 plants at 60 DAE vs. 90 DAE **(Supplementary Table 1)**. The mucilage fungal microbiome
427 structure was strongly influenced by year of collection (PERMANOVA R-squared= 0.51, $p <$
428 0.001). Fungal community structure was weakly influenced by developmental stage
429 (PERMANOVA R-squared= 0.02, $p < 0.05$), but not by fertilization status (PERMANOVA, $p >$
430 0.05) **(Figure 2C).**
431 The mucilage fungal microbiome was dominated by the Ascomycota (76%) and
432 Basidiomycota (23.7%) phyla. The Dothideomycetes (50%), Sordariomycetes (24%), and
433 Tremellomycetes (14%) fungal classes were the most abundant. Cladosporium (22%),
434 Nectriaceae (17%), Didymellaceae (14%), Bulleribasidiaceae (9 %), Pleosporaceae (8%) were
435 the dominant fungal families in the mucilage. The genera *Cladosporium* exhibited higher
436 abundance in the 2020 growing season (34%) compared with 2021 (14%). In contrast, we found

437 an enrichment of the genera *Epicoccum* in 2021 (18%) compared with the 2020 growing season
438 (0.02%) **(Supplementary Figure 1)**. Taking these results together, Hypothesis 4 was not
439 supported because the bacterial microbiome of mucilage was more sensitive to plant
440 development and consistent across sampling years than the fungal, while the fungal microbiome
441 also exhibited greater variability between years.
442
443 **Cultivation-dependent bacterial taxonomic and phenotypic diversity of sorghum**
444 **phyllosphere wax and mucilage**.
445 Bacterial culture collections from the epicuticular wax and aerial root mucilage were constructed
446 by enriching bacteria with putative plant-beneficial traits **(Table 1)**. In total, 500 bacteria from
447 the wax and 800 bacteria from the mucilage were isolated, and then a subset of 200 isolates from
448 both the wax and mucilage were taxonomically identified by sequencing the full-length 16S
449 rRNA gene (**Supplementary Table 2**). These isolates were chosen to represent the range of
450 different cultivation conditions employed and, additionally, to maximize distinguishing
451 phenotypes (morphology, color, etc) to avoid redundancy in the collection (**Figure 5**). The wax
452 bacterial collection was dominated by the Proteobacteria, followed by Actinobacteria, and
453 Bacteroidetes phyla, and the mucilage bacterial collection was dominated by the Proteobacteria,
454 followed by Actinobacteria, Firmicutes, and Bacteroidetes phyla **(Supplementary Table 2)**.
455 Forty-eight ASVs matched with 100% sequence identity to strains in the isolate
456 collections **(Supplementary Table 2)**. Most of the bacterial families found in the sorghum wax
457 and mucilage had representatives among the isolate collection **(Figure 6)**. Families such as
458 Beijerincklaceae, Chitinophagaceae, Oxalobacteraceae were not captured by our wax bacterial

459 cultivation efforts. Families observed using cultivation-independent techniques but that were not
460 captured by our mucilage cultivation efforts included Cytophagaceae and Oxalobacteraceae.
461 To understand potential novelty and redundancy represented by the diversity of our wax
462 and mucilage bacterial collections, we compared the full-length 16S rRNA genes with those
463 extracted from the bacterial genomes of previously described non-root-associated, plant-
464 associated (PA) bacteria (Levy et al. 2017), assigned as non-root-associated. 637 bacterial
465 genomes were retrieved from a publicly available database **(**see Methods**)** to provide a reference
466 of context for our 200 sorghum phyllosphere isolates. The final data set contained 527 non-
467 redundant full-length 16S rRNA sequences: 94 new 16S rRNA genes from our sorghum wax and
468 mucilage collections, and 433 rRNA genes from the published plant-associated bacterial
469 genomes (**Figure 7**).
470
471 **DISCUSSION**
472 We investigated the microbiota associated with bioenergy sorghum phyllosphere
473 exudates, specifically from epicuticular wax on stems and leaves and from mucilage on aerial
474 roots.
475 The chemistry of epicuticular wax that covers sorghum stems has been extensively
476 characterized (Bianchi et al. 1978; Jordan et al. 1984; Jenks et al. 2000; Farber et al. 2019a,
477 2019b), but there is still much to learn about its microbial residents and their colonization
478 dynamics. Thus, we decided to characterize the wax microbiota from stems of field-grown
479 bioenergy sorghum plants at 60 DAE and 90 DAE. We chose these two-time points because they
480 represent different developmental stages, and, in our field conditions, they also had different
481 water availability. During the vegetative stage, sorghum plants at 60 DAE have all leaves

482 developed and fully expanded. At 90 DAE in the upper mid-west, plants have transitioned to the
483 reproductive stage, seed development is in progress and nutrients are being relocated to the
484 kernel. In the southwestern U.S., sorghum plants are in extended vegetative growth stage, with
485 floral initiation expected at 120 DAE. The major lineages we detected in the epicuticular stem
486 wax, including *Proteobacteria*, *Bacteroidetes*, and *Actinobacteria,* agree generally with reports
487 from *Arabidopsis thaliana* and *Sorghum bicolor* epicuticular leaf wax (Reisberg et al. 2013; Sun
488 et al. 2021). Furthermore, we also observed changes in the relative abundances of several taxa at
489 60 DAE compared with plants at 90 DAE, which could be associated with changes in the
490 composition of the epicuticular wax as the plant grows (Avato et al. 1984; Jenks et al. 1996),
491 though more work is needed to characterize changes in the chemical composition of the wax
492 alongside the structural changes in the microbiome to understand their relationship more fully. It
493 has been suggested that microbes in wax may be able to metabolize wax components and use
494 them as a carbon source (Ueda et al. 2015). Our study enriched several bacterial isolates that
495 were able to grow with linalool and beta-caryophyllene, two of the terpenes found in sorghum
496 wax. To gain further insight into epicuticular wax microbiome assembly and dynamics, next
497 steps could expand this research not only by including samples from different growing seasons,
498 but also by including sorghum genotypes that are mutants in wax production (Jenks et al. 1994,
499 2000; Peters et al. 2009; Punnuri et al. 2017).

500 For decades it has been suggested that the sorghum aerial root mucilage harbors
501 diazotroph bacteria (Wani 1986; Bennett et al. 2020). We hypothesized that fertilization would
502 strongly influence the phyllosphere mucilage microbiota due to changes in exogenous nutrient
503 availability and changes in mucilage polysaccharide composition. However, our cultivation-
504 independent data (16S rRNA amplicons) suggest that that differences in nitrogen fertilization had

505 no notable influence on the microbiome structure for both bacterial and fungal communities. In
506 contrast, plant developmental stage strongly affected the mucilage bacterial microbiome
507 structure. Similar evidence of microbiome seasonality has been found in other studies of
508 different surfaces of the phyllosphere microbiome (Copeland et al. 2015; Grady et al. 2019;
509 Xiong et al. 2021; Smets et al. 2022). We also observed several putative diazotroph bacteria in
510 the sorghum mucilage that were isolated anaerobically and on nitrogen-free media, including
511 *Curtobacterium*, *Pantoea, Pseudomonas, Strenotrophomonas*, which were reported as lineages
512 that could colonize the maize mucilage (van Deynze et al. 2018; Higdon et al. 2020b, 2020a).
513 Regarding the fungal microbiome in the mucilage, we found that the year of collection
514 had the highest explanatory value. With two years of field data, there is not enough information
515 to understand if the fungal community is responsive to other covariates (e.g., weather) or more
516 stochastically assembled every year. Fungal community members likely have different
517 responses than bacterial members to changing environmental conditions, including temperature,
518 moisture, solar radiation, and precipitation (Jackson and Denney 2011; Copeland et al. 2015;
519 Wagner et al. 2016; Gomes et al. 2018). We can deduce that the bacterial and fungal
520 communities did not have strong relationships or co-dependencies based on their structures, and
521 likely have different dominating drivers. However, the possibility of redundant functional
522 relationships between different bacterial and fungal mucilage members cannot be eliminated.
523 We combined both culture-independent and dependent approaches to improve our
524 understanding of the microbiome diversity in phyllosphere exudates. Due to the chemical
525 composition, plant DNA contamination, and low bacterial biomass associated with the wax and
526 mucilage, a metagenomic sequencing approach would have been challenging to pursue with the
527 sorghum phyllosphere (Sharpton 2014; van Deynze et al. 2018). Sequencing the V4 16S rRNA

528 and the ITS1 regions allowed us to deeply characterize bacterial and fungal communities in
529 sorghum phyllosphere exudates, albeit with limited taxonomic resolution that can be provided by
530 the amplicons (to approximately the genus level Poretsky et al. 2014) as well as limited
531 functional insight (Langille et al. 2013; Turner et al. 2013). Thus, we decided to culture wax and
532 mucilage bacteria by using a variety of isolation media and growing conditions that we expected
533 to enrich for plant-beneficial bacterial phenotypes. In the end, we were able to capture
534 representatives of most of the bacterial families and genera that we observed in our culture-
535 independent approach. These isolates can now be used to test directly for plant beneficial
536 properties and microbe-plant interactions in the laboratory.

537 In summary, we report a characterization of microbiome structure of energy sorghum
538 phyllosphere exudates, epicuticular wax and aerial root mucilage under multiple field conditions
539 and across two seasons for mucilage. We found that the wax and mucilage harbor distinct
540 bacterial communities, suggesting niche specialization in the sorghum phyllosphere, and
541 captured several key bacterial lineages in a parallel cultivation effort. Additionally, we found that
542 fungal communities and bacterial communities in the mucilage are responsive to different
543 drivers, with bacterial communities most distinctive by developmental stage and fungal
544 communities most distinctive by year of sample collection. Next steps are to use the ecological
545 dynamics from the cultivation-independent sequencing and apparent phenotypes of the bacterial
546 isolates to understand the roles of these exudate microbiome members for plant performance.
547

548 **ACKNOWLEDGMENTS**

549 This work was supported by the Great Lakes Bioenergy Research Center, U.S. Department of
550 Energy, Office of Science, Office of Biological and Environmental Research under Award

551 Number DE-SC0018409. Support for field research was provided by the Great Lakes Bioenergy
552 Research Center, U.S. Department of Energy, Office of Science, Office of Biological and
553 Environmental Research (Awards DE-SC0018409 and DE-FC02-07ER64494), by the National
554 Science Foundation Long-term Ecological Research Program (DEB 1637653) at the Kellogg
555 Biological Station, and by Michigan State University AgBioResearch. JM acknowledges field
556 support from graduate students at TAMU. AS acknowledges support from Michigan State
557 University AgBioResearch.

558

559 The authors declare no conflict of interest.

560

561 **LITERATURE CITED**

562 Amicucci, M. J., Galermo, A. G., Guerrero, A., Treves, G., Nandita, E., Kailemia, M. J., et al.
563 2019. Strategy for Structural Elucidation of Polysaccharides: Elucidation of a Maize
564 Mucilage that Harbors Diazotrophic Bacteria. Anal Chem. 91:7254–7265 Available at:
565 https://doi.org/10.1021/acs.analchem.9b00789.
566 Avato, P., Bianchi, G., and Mariani, G. 1984. Epicuticular waxes of Sorghum and some
567 compositional changes with plant age. Phytochemistry. 23:2843–2846 Available at:
568 https://www.sciencedirect.com/science/article/pii/0031942284830265.
569 Beattie, G. A., and Marcell, L. M. 2002. Effect of alterations in cuticular wax biosynthesis on the
570 physicochemical properties and topography of maize leaf surfaces. Plant Cell Environ.
571 25:1–16.
572 Bennett, A. B., Pankievicz, V. C. S., and Ané, J.-M. 2020. A Model for Nitrogen Fixation in
573 Cereal Crops. Trends Plant Sci. 25:226–235 Available at:
574 https://www.sciencedirect.com/science/article/pii/S1360138519303292.
575 Bianchi, G., Avato, P., Bertorelli, P., and Mariani, G. 1978. Epicuticular waxes of two sorghum
576 varieties. Phytochemistry. 17:999–1001 Available at:
577 https://www.sciencedirect.com/science/article/pii/S0031942200886689.
578 Bolyen, E., Rideout, J. R., Dillon, M. R., Bokulich, N. A., Abnet, C. C., Al-Ghalith, G. A., et al.
579 2019. Reproducible, interactive, scalable and extensible microbiome data science using
580 QIIME 2. Nat Biotechnol. 37:852–857 Available at: https://doi.org/10.1038/s41587-019-
581 0209-9.
582 Bondada, B. R., Oosterhuis, D. M., Murphy, J. B., and Kim, K. S. 1996. Effect of water stress on
583 the epicuticular wax composition and ultrastructure of cotton (Gossypium hirsutum L.)
584 leaf, bract, and boll. Environ Exp Bot. 36:61–69 Available at:
585 https://www.sciencedirect.com/science/article/pii/0098847296001281.

586 Busta, L., Schmitz, E., Kosma, D. K., Schnable, J. C., and Cahoon, E. B. 2021. A co-opted
587 steroid synthesis gene, maintained in sorghum but not maize, is associated with a
588 divergence in leaf wax chemistry. Proceedings of the National Academy of Sciences.
589 118:e2022982118 Available at: https://doi.org/10.1073/pnas.2022982118.
590 Callahan, B. J., McMurdie, P. J., Rosen, M. J., Han, A. W., Johnson, A. J. A., and Holmes, S. P.
591 2016. DADA2: High-resolution sample inference from Illumina amplicon data. Nat
592 Methods. 13:581–583 Available at: https://doi.org/10.1038/nmeth.3869.
593 Capella-Gutiérrez, S., Silla-Martínez, J. M., and Gabaldón, T. 2009. trimAl: a tool for automated
594 alignment trimming in large-scale phylogenetic analyses. Bioinformatics. 25:1972–1973
595 Available at: https://doi.org/10.1093/bioinformatics/btp348.
596 Caporaso, G. J., Lauber, C. L., Walters, W., Berg-Lyons, D., Lozupone, C. A., Turnbaugh, P.J.,
597 et al. 2011. Global patterns of 16S rRNA diversity at a depth of millions of sequences per
598 sample. Proceedings of the National Academy of Sciences. 108:4516–4522 Available at:
599 https://doi.org/10.1073/pnas.1000080107.
600 Chai, Y. N., and Schachtman, D. P. 2022. Root exudates impact plant performance under abiotic
601 stress. Trends Plant Sci. 27:80–91 Available at:
602 https://doi.org/10.1016/j.tplants.2021.08.003.
603 Copeland, J. K., Yuan, L., Layeghifard, M., Wang, P. W., and Guttman, D. S. 2015. Seasonal
604 Community Succession of the Phyllosphere Microbiome. Molecular Plant-Microbe
605 Interactions®. 28:274–285 Available at: https://doi.org/10.1094/MPMI-10-14-0331-FI.
606 van Deynze, A., Zamora, P., Delaux, P.-M., Heitmann, C., Jayaraman, D., Rajasekar, S., et al.
607 2018. Nitrogen fixation in a landrace of maize is supported by a mucilage-associated
608 diazotrophic microbiota. PLoS Biol. 16:e2006352- Available at:
609 https://doi.org/10.1371/journal.pbio.2006352.
610 Dixon, P. 2003. VEGAN, A Package of R Functions for Community Ecology. Journal of
611 Vegetation Science. 14:927–930 Available at: http://www.jstor.org/stable/3236992.
612 Doan, H. K., Ngassam, V. N., Gilmore, S. F., Tecon, R., Parikh, A. N., and Leveau, J. H. J.
613 2020. Topography-Driven Shape, Spread, and Retention of Leaf Surface Water Impacts
614 Microbial Dispersion and Activity in the Phyllosphere. Phytobiomes J. 4:268–280
615 Available at: https://doi.org/10.1094/PBIOMES-01-20-0006-R.
616 Farber, C., Li, J., Hager, E., Chemelewski, R., Mullet, J., Rogachev, A. Y., et al. 2019a.
617 Complementarity of Raman and Infrared Spectroscopy for Structural Characterization of
618 Plant Epicuticular Waxes. ACS Omega. 4:3700–3707 Available at:
619 https://doi.org/10.1021/acsomega.8b03675.
620 Farber, C., Wang, R., Chemelewski, R., Mullet, J., and Kurouski, D. 2019b. Nanoscale Structural
621 Organization of Plant Epicuticular Wax Probed by Atomic Force Microscope Infrared
622 Spectroscopy. Anal Chem. 91:2472–2479 Available at:
623 https://doi.org/10.1021/acs.analchem.8b05294.
624 Galloway, A. F., Knox, P., and Krause, K. 2020. Sticky mucilages and exudates of plants:
625 putative microenvironmental design elements with biotechnological value. New
626 Phytologist. 225:1461–1469 Available at: https://doi.org/10.1111/nph.16144.
627 Gomes, T., Pereira, J. A., Benhadi, J., Lino-Neto, T., and Baptista, P. 2018. Endophytic and
628 Epiphytic Phyllosphere Fungal Communities Are Shaped by Different Environmental
629 Factors in a Mediterranean Ecosystem. Microb Ecol. 76:668–679 Available at:
630 https://doi.org/10.1007/s00248-018-1161-9.

631 Grady, K. L., Sorensen, J. W., Stopnisek, N., Guittar, J., and Shade, A. 2019. Assembly and
632 seasonality of core phyllosphere microbiota on perennial biofuel crops. Nat Commun.
633 10:4135 Available at: https://doi.org/10.1038/s41467-019-11974-4.
634 Higdon, S. M., Pozzo, T., Kong, N., Huang, B. C., Yang, M. L., Jeannotte, R., et al. 2020a.
635 Genomic characterization of a diazotrophic microbiota associated with maize aerial root
636 mucilage. PLoS One. 15:e0239677- Available at:
637 https://doi.org/10.1371/journal.pone.0239677.
638 Higdon, S. M., Pozzo, T., Tibbett, E. J., Chiu, C., Jeannotte, R., Weimer, B. C., et al. 2020b.
639 Diazotrophic bacteria from maize exhibit multifaceted plant growth promotion traits in
640 multiple hosts. PLoS One. 15:e0239081- Available at:
641 https://doi.org/10.1371/journal.pone.0239081.
642 Hoang, D. T., Chernomor, O., von Haeseler, A., Minh, B. Q., and Vinh, L. S. 2018. UFBoot2:
643 Improving the Ultrafast Bootstrap Approximation. Mol Biol Evol. 35:518–522 Available
644 at: https://doi.org/10.1093/molbev/msx281.
645 Jackson, C. R., and Denney, W. C. 2011. Annual and Seasonal Variation in the Phyllosphere
646 Bacterial Community Associated with Leaves of the Southern Magnolia (Magnolia
647 grandiflora). Microb Ecol. 61:113–122 Available at: https://doi.org/10.1007/s00248-010-
648 9742-2.
649 Jenks, M. A., Joly, R. J., Peters, P. J., Rich, P. J., Axtell, J. D., and Ashworth, E. N. 1994.
650 Chemically Induced Cuticle Mutation Affecting Epidermal Conductance to Water Vapor
651 and Disease Susceptibility in Sorghum bicolor (L.) Moench. Plant Physiol. 105:1239–
652 1245 Available at: https://pubmed.ncbi.nlm.nih.gov/12232280.
653 Jenks, M. A., Rich, P. J., Rhodes, D., Ashworth, E. N., Axtell, J. D., and Ding, C.-K. 2000. Leaf
654 sheath cuticular waxes on bloomless and sparse-bloom mutants of Sorghum bicolor.
655 Phytochemistry. 54:577–584 Available at:
656 https://www.sciencedirect.com/science/article/pii/S0031942200001539.
657 Jenks, M. A., Tuttle, H. A., and Feldmann, K. A. 1996. Changes in epicuticular waxes on
658 wildtype and eceriferum mutants in Arabidopsis during development. Phytochemistry.
659 42:29–34 Available at:
660 https://www.sciencedirect.com/science/article/pii/0031942295008985.
661 Jordan, W. R., Shouse, P. J., Blum, A., Miller, F. R., and Monk, R. L. 1984. Environmental
662 Physiology of Sorghum. II. Epicuticular Wax Load and Cuticular Transpiration1. Crop
663 Sci. 24:cropsci1984.0011183X002400060038x Available at:
664 https://doi.org/10.2135/cropsci1984.0011183X002400060038x.
665 Kalyaanamoorthy, S., Minh, B. Q., Wong, T. K. F., von Haeseler, A., and Jermiin, L. S. 2017.
666 ModelFinder: fast model selection for accurate phylogenetic estimates. Nat Methods.
667 14:587–589 Available at: https://pubmed.ncbi.nlm.nih.gov/28481363.
668 Katoh, K., Misawa, K., Kuma, K., and Miyata, T. 2002. MAFFT: a novel method for rapid
669 multiple sequence alignment based on fast Fourier transform. Nucleic Acids Res.
670 30:3059–3066 Available at: https://doi.org/10.1093/nar/gkf436.
671 Kent, J., Hartman, M. D., Lee, D. K., and Hudiburg, T. 2020. Simulated Biomass Sorghum GHG
672 Reduction Potential is Similar to Maize. Environ Sci Technol. 54:12456–12466 Available
673 at: https://doi.org/10.1021/acs.est.0c01676.
674 Ku, L. X., Sun, Z. H., Wang, C. L., Zhang, J., Zhao, R. F., Liu, H. Y., et al. 2012. QTL mapping
675 and epistasis analysis of brace root traits in maize. Molecular Breeding. 30:697–708
676 Available at: https://doi.org/10.1007/s11032-011-9655-x.

677 Kunst, L., and Samuels, A. L. 2003. Biosynthesis and secretion of plant cuticular wax. Prog
678 Lipid Res. 42:51–80 Available at:
679 https://www.sciencedirect.com/science/article/pii/S0163782702000450.
680 Langille, M. G. I., Zaneveld, J., Caporaso, J. G., McDonald, D., Knights, D., Reyes, J. A., et al.
681 2013. Predictive functional profiling of microbial communities using 16S rRNA marker
682 gene sequences. Nat Biotechnol. 31:814–821 Available at:
683 https://doi.org/10.1038/nbt.2676.
684 Letunic, I., and Bork, P. 2021. Interactive Tree Of Life (iTOL) v5: an online tool for
685 phylogenetic tree display and annotation. Nucleic Acids Res. 49:W293–W296 Available
686 at: https://doi.org/10.1093/nar/gkab301.
687 Levy, A., Salas Gonzalez, I., Mittelviefhaus, M., Clingenpeel, S., Herrera Paredes, S., Miao, J.,
688 et al. 2017. Genomic features of bacterial adaptation to plants. Nat Genet. 50:138–150
689 Available at: https://pubmed.ncbi.nlm.nih.gov/29255260.
690 Li, W., and Godzik, A. 2006. Cd-hit: a fast program for clustering and comparing large sets of
691 protein or nucleotide sequences. Bioinformatics. 22:1658–1659 Available at:
692 https://doi.org/10.1093/bioinformatics/btl158.
693 Lindow, S. E., and Brandl, M. T. 2003. Microbiology of the phyllosphere. Appl Environ
694 Microbiol. 69:1875–1883 Available at: https://pubmed.ncbi.nlm.nih.gov/12676659.
695 Love, M. I., Huber, W., and Anders, S. 2014. Moderated estimation of fold change and
696 dispersion for RNA-seq data with DESeq2. Genome Biol. 15:550 Available at:
697 https://doi.org/10.1186/s13059-014-0550-8.
698 McMurdie, P. J., and Holmes, S. 2013. phyloseq: An R Package for Reproducible Interactive
699 Analysis and Graphics of Microbiome Census Data. PLoS One. 8:e61217- Available at:
700 https://doi.org/10.1371/journal.pone.0061217.
701 Miller, C. S., Handley, K. M., Wrighton, K. C., Frischkorn, K. R., Thomas, B. C., and Banfield,
702 J. F. 2013. Short-Read Assembly of Full-Length 16S Amplicons Reveals Bacterial
703 Diversity in Subsurface Sediments. PLoS One. 8:e56018- Available at:
704 https://doi.org/10.1371/journal.pone.0056018.
705 Minh, B. Q., Schmidt, H. A., Chernomor, O., Schrempf, D., Woodhams, M. D., von Haeseler,
706 A., et al. 2020. IQ-TREE 2: New Models and Efficient Methods for Phylogenetic
707 Inference in the Genomic Era. Mol Biol Evol. 37:1530–1534 Available at:
708 https://doi.org/10.1093/molbev/msaa015.
709 Mullet, J., Morishige, D., McCormick, R., Truong, S., Hilley, J., McKinley, B., et al. 2014.
710 Energy Sorghum—a genetic model for the design of C4 grass bioenergy crops. J Exp
711 Bot. 65:3479–3489 Available at: https://doi.org/10.1093/jxb/eru229.
712 Nazari, M., Riebeling, S., Banfield, C. C., Akale, A., Crosta, M., Mason-Jones, K., et al. 2020.
713 Mucilage Polysaccharide Composition and Exudation in Maize From Contrasting
714 Climatic Regions. Front Plant Sci. 11 Available at:
715 https://www.frontiersin.org/article/10.3389/fpls.2020.587610.
716 Nilsson, R. H., Larsson, K.-H., Taylor, A. F. S., Bengtsson-Palme, J., Jeppesen, T. S., Schigel,
717 D., et al. 2019. The UNITE database for molecular identification of fungi: handling dark
718 taxa and parallel taxonomic classifications. Nucleic Acids Res. 47:D259–D264 Available
719 at: https://doi.org/10.1093/nar/gky1022.
720 Olson, S. N., Ritter, K., Rooney, W., Kemanian, A., McCarl, B. A., Zhang, Y., et al. 2012. High
721 biomass yield energy sorghum: developing a genetic model for C4 grass bioenergy crops.

722 Biofuels, Bioproducts and Biorefining. 6:640–655 Available at:
723 https://doi.org/10.1002/bbb.1357.
724 Peters, P. J., Jenks, M. A., Rich, P. J., Axtell, J. D., and Ejeta, G. 2009. Mutagenesis, Selection,
725 and Allelic Analysis of Epicuticular Wax Mutants in Sorghum. Crop Sci. 49:1250–1258
726 Available at: https://doi.org/10.2135/cropsci2008.08.0461.
727 Pierce, M. P. 2019. The ecological and evolutionary importance of nectar-secreting galls.
728 Ecosphere. 10:e02670 Available at: https://doi.org/10.1002/ecs2.2670.
729 Poretsky, R., Rodriguez-R, L. M., Luo, C., Tsementzi, D., and Konstantinidis, K. T. 2014.
730 Strengths and Limitations of 16S rRNA Gene Amplicon Sequencing in Revealing
731 Temporal Microbial Community Dynamics. PLoS One. 9:e93827- Available at:
732 https://doi.org/10.1371/journal.pone.0093827.
733 Punnuri, S., Harris-Shultz, K., Knoll, J., Ni, X., and Wang, H. 2017. The Genes Bm2 and Blmc
734 that Affect Epicuticular Wax Deposition in Sorghum are Allelic. Crop Sci. 57:1552–1556
735 Available at: https://doi.org/10.2135/cropsci2016.11.0937.
736 Quast, C., Pruesse, E., Yilmaz, P., Gerken, J., Schweer, T., Yarza, P., et al. 2013. The SILVA
737 ribosomal RNA gene database project: improved data processing and web-based tools.
738 Nucleic Acids Res. 41:D590–D596 Available at: https://doi.org/10.1093/nar/gks1219.
739 Reisberg, E. E., Hildebrandt, U., Riederer, M., and Hentschel, U. 2013. Distinct phyllosphere
740 bacterial communities on Arabidopsis wax mutant leaves. PLoS One. 8:e78613–e78613
741 Available at: https://pubmed.ncbi.nlm.nih.gov/24223831.
742 Reneau, J. W., Khangura, R. S., Stager, A., Erndwein, L., Weldekidan, T., Cook, D. D., et al.
743 2020. Maize brace roots provide stalk anchorage. Plant Direct. 4:e00284 Available at:
744 https://doi.org/10.1002/pld3.284.
745 Rering, C. C., Beck, J. J., Hall, G. W., McCartney, M. M., and Vannette, R. L. 2018. Nectar-
746 inhabiting microorganisms influence nectar volatile composition and attractiveness to a
747 generalist pollinator. New Phytologist. 220:750–759 Available at:
748 https://doi.org/10.1111/nph.14809.
749 Ruinen, J. 1965. The phyllosphere. Plant Soil. 22:375–394 Available at:
750 https://doi.org/10.1007/BF01422435.
751 Scully, M. J., Norris, G. A., Alarcon Falconi, T. M., and MacIntosh, D. L. 2021. Carbon intensity
752 of corn ethanol in the United States: state of the science. Environmental Research Letters.
753 16:043001 Available at: http://dx.doi.org/10.1088/1748-9326/abde08.
754 Seemann, T. 2014. Prokka: rapid prokaryotic genome annotation. Bioinformatics. 30:2068–2069
755 Available at: https://doi.org/10.1093/bioinformatics/btu153.
756 Serrano, M., Coluccia, F., Torres, M., L'Haridon, F., and Métraux, J.-P. 2014. The cuticle and
757 plant defense to pathogens. Front Plant Sci. 5:274 Available at:
758 https://pubmed.ncbi.nlm.nih.gov/24982666.
759 Sharpton, T. J. 2014. An introduction to the analysis of shotgun metagenomic data. Front Plant
760 Sci. 5 Available at: https://www.frontiersin.org/article/10.3389/fpls.2014.00209.
761 Shepherd, T., Robertson, G. W., Griffiths, D. W., Birch, A. N. E., and Duncan, G. 1995. Effects
762 of environment on the composition of epicuticular wax from kale and swede.
763 Phytochemistry. 40:407–417 Available at:
764 https://www.sciencedirect.com/science/article/pii/003194229500281B.
765 Shepherd, T., and Wynne Griffiths, D. 2006. The effects of stress on plant cuticular waxes. New
766 Phytologist. 171:469–499 Available at: https://doi.org/10.1111/j.1469-
767 8137.2006.01826.x.

768 Smets, W., Spada, M. L., Gandolfi, I., Wuyts, K., Legein, M., Muyshondt, B., et al. 2022.
769 Bacterial Succession and Community Dynamics of the Emerging Leaf Phyllosphere in
770 Spring. Microbiol Spectr. 10:e02420-21 Available at:
771 https://doi.org/10.1128/spectrum.02420-21.
772 Stamp, P., and Kiel, C. 1992. Root Morphology of Maize and Its Relationship to Root Lodging. J
773 Agron Crop Sci. 168:113–118 Available at: https://doi.org/10.1111/j.1439-
774 037X.1992.tb00987.x.
775 Steinmüller, D., and Tevini, M. 1985. Action of ultraviolet radiation (UV-B) upon cuticular
776 waxes in some crop plants. Planta. 164:557–564 Available at:
777 https://doi.org/10.1007/BF00395975.
778 Sun, A., Jiao, X.-Y., Chen, Q., Wu, A.-L., Zheng, Y., Lin, Y.-X., et al. 2021. Microbial
779 communities in crop phyllosphere and root endosphere are more resistant than soil
780 microbiota to fertilization. Soil Biol Biochem. 153:108113 Available at:
781 https://www.sciencedirect.com/science/article/pii/S0038071720304090.
782 Tsuba, M., Katagiri, C., Takeuchi, Y., Takada, Y., and Yamaoka, N. 2002. Chemical factors of
783 the leaf surface involved in the morphogenesis of Blumeria graminis. Physiol Mol Plant
784 Pathol. 60:51–57 Available at:
785 https://www.sciencedirect.com/science/article/pii/S0885576502903760.
786 Turner, T. R., James, E. K., and Poole, P. S. 2013. The plant microbiome. Genome Biol. 14:209
787 Available at: https://doi.org/10.1186/gb-2013-14-6-209.
788 Ueda, H., Mitsuhara, I., Tabata, J., Kugimiya, S., Watanabe, T., Suzuki, K., et al. 2015.
789 Extracellular esterases of phylloplane yeast Pseudozyma antarctica induce defect on
790 cuticle layer structure and water-holding ability of plant leaves. Appl Microbiol
791 Biotechnol. 99:6405–6415 Available at: https://doi.org/10.1007/s00253-015-6523-3.
792 Vacher, C., Hampe, A., Porté, A. J., Sauer, U., Compant, S., and Morris, C. E. 2016. The
793 Phyllosphere: Microbial Jungle at the Plant–Climate Interface. Annu Rev Ecol Evol Syst.
794 47:1–24 Available at: https://doi.org/10.1146/annurev-ecolsys-121415-032238.
795 Varoquaux, N., Cole, B., Gao, C., Pierroz, G., Baker, C. R., Patel, D., et al. 2019. Transcriptomic
796 analysis of field-droughted sorghum from seedling to maturity reveals biotic and
797 metabolic responses. Proceedings of the National Academy of Sciences. 116:27124–
798 27132 Available at: https://doi.org/10.1073/pnas.1907500116.
799 Vorholt, J. A. 2012. Microbial life in the phyllosphere. Nat Rev Microbiol. 10:828–840
800 Available at: https://doi.org/10.1038/nrmicro2910.
801 Wagner, M. R., Lundberg, D. S., del Rio, T. G., Tringe, S. G., Dangl, J. L., and Mitchell-Olds, T.
802 2016. Host genotype and age shape the leaf and root microbiomes of a wild perennial
803 plant. Nat Commun. 7:12151 Available at: https://doi.org/10.1038/ncomms12151.
804 Wani, S. 1986. Cereal nitrogen fixation: Proceedings of the Working Group meeting held at
805 ICRISAY Center, India, 9-12 October 1984. Available at: http://oar.icrisat.org/851/
806 Wang, X., Kong, L., Zhi, P., and Chang, C. 2020. Update on Cuticular Wax Biosynthesis and Its
807 Roles in Plant Disease Resistance. Int J Mol Sci. 21:5514 Available at:
808 https://pubmed.ncbi.nlm.nih.gov/32752176.
809 Weinstein, M. M., Prem, A., Jin, M., Tang, S., and Bhasin, J. M. 2019. FIGARO: An efficient
810 and objective tool for optimizing microbiome rRNA gene trimming parameters. bioRxiv.
811 :610394 Available at: http://biorxiv.org/content/early/2019/04/16/610394.abstract.

812 von Wettstein-Knowles, P. 1974. Ultrastructure and origin of epicuticular wax tubes. J
813 Ultrastruct Res. 46:483–498 Available at:
814 https://www.sciencedirect.com/science/article/pii/S0022532074900690.
815 Xiong, C., Singh, B. K., He, J.-Z., Han, Y.-L., Li, P.-P., Wan, L.-H., et al. 2021. Plant
816 developmental stage drives the differentiation in ecological role of the maize
817 microbiome. Microbiome. 9:171 Available at: https://doi.org/10.1186/s40168-021-
818 01118-6.
819 Xue, D., Zhang, X., Lu, X., Chen, G., and Chen, Z.-H. 2017. Molecular and Evolutionary
820 Mechanisms of Cuticular Wax for Plant Drought Tolerance. Front Plant Sci. 8:621
821 Available at: https://pubmed.ncbi.nlm.nih.gov/28503179.
822 Yeats, T. H., and Rose, J. K. C. 2013. The formation and function of plant cuticles. Plant
823 Physiol. 163:5–20 Available at: https://pubmed.ncbi.nlm.nih.gov/23893170.
824

825

826 **TABLES**

827 **Table 1.** Solid media and their enrichment objectives (target phenotypes) used in this study to
828 culture bacteria from the sorghum wax and mucilage. Dilutions from 10^{-1} to 10^{-4} were plated for
829 each condition, for each exudate.

830

Media	Target phenotype	Temperature (°C)	Oxygen condition
Reasoner's 2A agar (R2A)	General diversity	25, 37	Aerobic, anaerobic
50% R2A	General diversity	25, 37	Aerobic, anaerobic
Tryptic Soy Agar (TSA)	General diversity	25, 37	Aerobic, anaerobic
50% TSA	General diversity	25, 37	Aerobic, anaerobic
M9 minimal medium	General diversity	25, 37	Aerobic, anaerobic
King's B medium	*Pseudomonas* species	25, 37	Aerobic, anaerobic
Nitrogen-free Jensen's medium	Nitrogen fixation	25, 37	Aerobic, anaerobic
M9 minimal medium nitrogen-free, 1% xylose	Nitrogen fixation	25, 37	Aerobic, anaerobic
M9 minimal medium nitrogen-free, 1% galactose	Nitrogen fixation	25, 37	Aerobic, anaerobic
M9 minimal medium nitrogen-free, 1% arabinose	Nitrogen fixation	25, 37	Aerobic, anaerobic
M9 minimal medium nitrogen-carbon free	Nitrogen fixation	25, 37	Aerobic, anaerobic
Pirovskaya's agar	Phosphate solubilization	25, 37	Aerobic, anaerobic
50% Tryptic Soy Broth, 1% linalool*	Resistance to/utilization of terpenoids	28	Aerobic
50% Tryptic Soy Broth, 1% β-caryophyllene*	Resistance to/utilization of terpenoids	28	Aerobic
50% Tryptic Soy Broth, 6000 Polyethylene Glycol*	Osmotic tolerance	28	Aerobic
Gauze's synthetic medium N-1	Actinobacteria species	25	Aerobic
Methanol Mineral Salts Medium	Methylotrophs	25	Aerobic

831 *After initial enrichment in liquid media, turbid cultures were diluted and plated onto R2A to isolate colonies.
832

833

834 **Table 2.** Sequencing summary of sorghum epicuticular wax and aerial root mucilage microbial

835 communities characterized in this study.

	Wax (16S rRNA) 2020	Mucilage (16S rRNA) 2020	Mucilage (16S rRNA) 2021	Mucilage (ITS1) 2020	Mucilage (ITS1) 2021
Number of samples	48	99	80	92	81
Raw Read Pairs	8,648,839	12,783,054	10,034,885	10,403,184	9,778,220
QC reads	7,930,768	10,809,135	9,071,499	6,200,571	5,957,248
% Chloroplast/ Mitochondria/ unassigned of QC reads	70%	24%	48%	0%	0%

836

837

838

839 **Table 3.** Permuted multivariate analysis of variance (PERMANOVA) to test for microbiome

840 differences in beta diversity.

Dataset	Exudate	Variable tested	Degrees of freedom	PseudoF	R-squared	*p*-value
Bacteria	Mucilage, wax	Exudate	1	35.51	0.14	<0.001
	Mucilage	Development	1	25.22	0.14	<0.001
	Mucilage	Fertilization	1	4.26	0.03	<0.001
	Mucilage	Year	1	3.36	0.02	<0.001
	Mucilage	Fertilization*Development	1	1.78	0.01	0.05
	Mucilage	Development*Year	1	2.78	0.01	<0.01
	Mucilage	Fertilization*Year	1	1.64	0.01	0.06
	Wax	Development	1	2.75	0.06	<0.01
Fungi	Mucilage	Development	1	3.25	0.02	<0.05
	Mucilage	Fertilization	1	2.20	0.01	0.07
	Mucilage	Year	1	176.38	0.51	<0.001
	Mucilage	Fertilization*Development	1	0.57	0.00	0.68
	Mucilage	Development*Year	1	5.03	0.01	<0.01
	Mucilage	Fertilization*Year	1	4.29	0.01	<0.05

841

842 **Figure Legends**

843 **Figure 1.** Sequencing effort and alpha diversity for sorghum epicuticular wax and aerial root
844 mucilage. Amplicon sequencing variants (ASVs) were defined at 100% identity of 16S rRNA
845 gene or ITS1 gene for bacterial and fungal datasets, respectively. Subsampled read depth is
846 indicated by the red, vertical, dashed line. Top panel: Rarefaction curves of quality-controlled
847 sequences. Bottom panels: Observed taxa (No. ASVs, *a.k.a.* richness) and phylogenetic diversity
848 (PD) metrics. A) Epicuticular wax bacterial samples were rarefied to 1,303 reads per sample. B)
849 Aerial root mucilage bacterial samples were rarefied to 20,519 reads per sample. C) Aerial root
850 mucilage fungal samples were rarefied to 33,975 reads per sample.

851

852 **Figure 2.** Relative abundances of bacterial families in sorghum epicuticular wax (A) and aerial
853 root mucilage (B) at 60 and 90 days after plant emergence; and relative abundances of fungal
854 families in mucilage (C) from samples collected in 2020 and 2021. Only families with relative
855 abundances >0.03 are shown.

856

857 **Figure 3.** Principal Coordinates Analysis (PCoA) based on Bray-Curtis dissimilarities for
858 bacterial microbiome from sorghum epicuticular wax (A), bacterial microbiome from aerial root
859 mucilage (B) and fungal microbiome from mucilage (C). DAE is days after plant emergence.

860

861 **Figure 4.** Differential abundance analysis for amplicon sequencing variants (ASVs) defined at
862 100% sequence identity. Differentially enriched bacterial ASVs in the aerial root mucilage of
863 plants at 60 and 90 DAE are shown. The fold change is shown on the x-axis and bacterial genera

are listed on the y-axis. Each colored dot represents a separate ASV annotated within a bacterial Class.

Figure 5. Taxonomic diversity of the subset of bacteria cultivated from sorghum epicuticular wax and aerial root mucilage that were selected for 16S rRNA gene sequence analysis based on representation of different cultivation conditions and colony phenotypes. A) Bacterial isolates cultured at 25°C under aerobic conditions, B) Bacterial isolates cultured at 37°C under aerobic conditions, C) Bacterial isolates cultured at 25°C under anaerobic conditions, and D) Bacterial isolates cultured at 37°C under anaerobic conditions.

Figure 6. Overlap in bacterial diversity found in the sorghum epicuticular wax and aerial root mucilage based on culture-independent and culture-dependent approaches. Relative abundance at the family level > 0.01 are shown.

Figure 7. Phylogenetic diversity in the sorghum epicuticular wax and aerial root mucilage. Maximum Likelihood phylogenetic tree (IQTREE, under UNREST+FO+I+G4 model) is based on the 16S rRNA gene alignment from nonredundant sorghum bacterial isolates and Levy et al. 2017 genomes.

882 **Supplementary Information**

883 **Supplementary Figure S1**. Relative abundances of bacterial genera in sorghum epicuticular
884 wax (A) and aerial root mucilage (B) at 60 and 90 days after plant emergence; and relative
885 abundances of fungal families in mucilage (C) from samples collected in 2020 and 2021. Only
886 genera with relative abundances >0.03 are shown.

887

888 **Supplementary Table S1**. *Excel file.* Tests for differences in bacterial and fungal alpha diversity
889 (richness, *a.k.a.* number of observed taxa) between exudates (mucilage, wax) and, within each
890 exudate, between categories of development (60 v. 90 DAE), fertilization (nitrogen-fertilized,
891 unfertilized), and year (2020, 2021) using the Wilcoxon rank sum test with continuity correction.

892

893 **Supplementary Table S2**. *Excel file.* Bacterial isolates from wax and mucilage and their
894 taxonomy based on full-length 16S rRNA gene Sanger sequencing. The isolates that shared
895 100% sequence identity to short-read bacterial ASVs (Amplicon Sequencing Variants) are
896 indicated and mapped to the ASV ID.

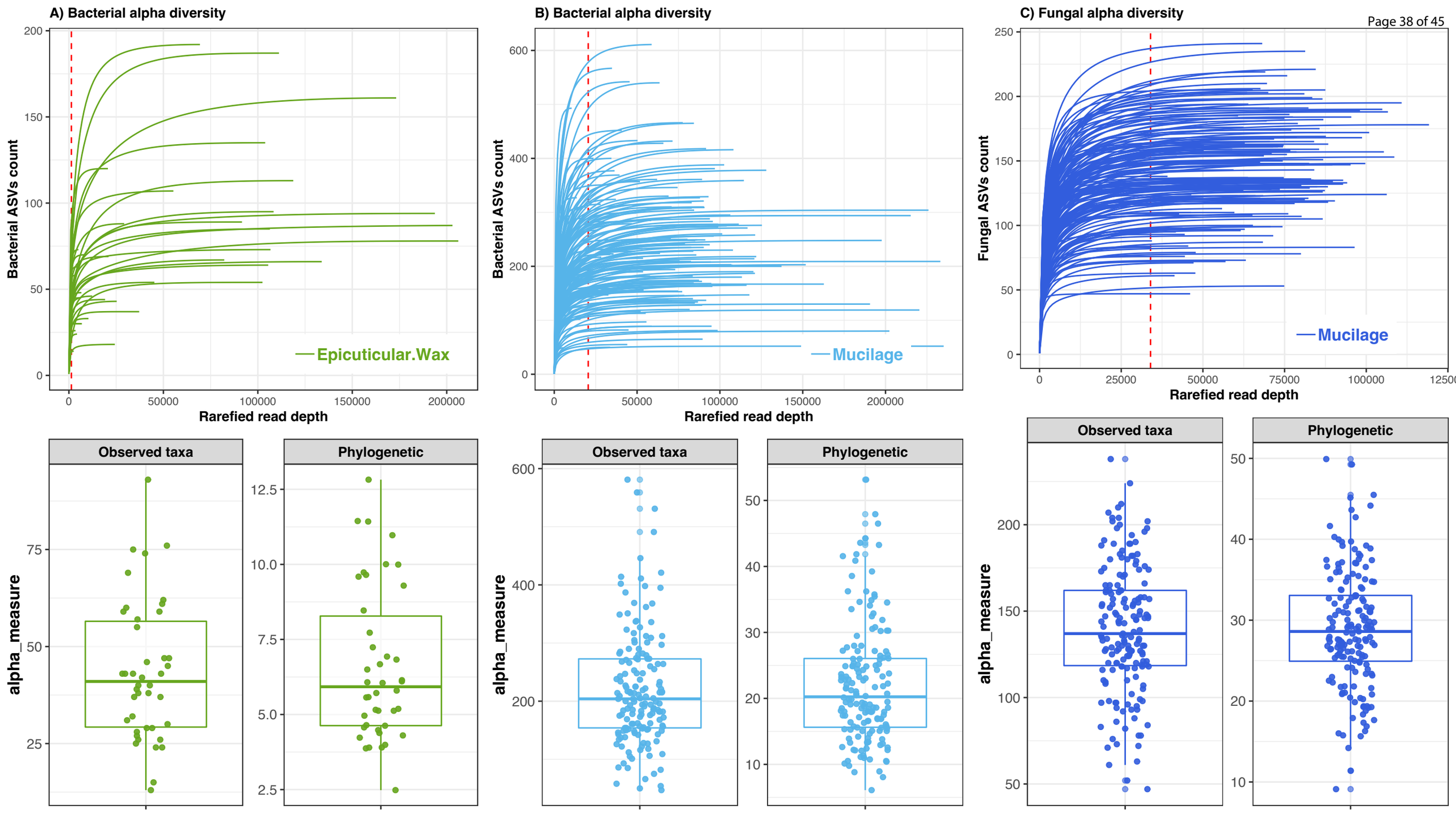
A) Bacterial alpha diversity
Bacterial ASVs count
Rarefied read depth
Epicuticular.Wax
B) Bacterial alpha diversity
Bacterial ASVs count
Rarefied read depth
Mucilage
C) Fungal alpha diversity
Fungal ASVs count
Rarefied read depth
Mucilage
Observed taxa
Phylogenetic
alpha_measure
Observed taxa
Phylogenetic
alpha_measure
Observed taxa
Phylogenetic
alpha_measure

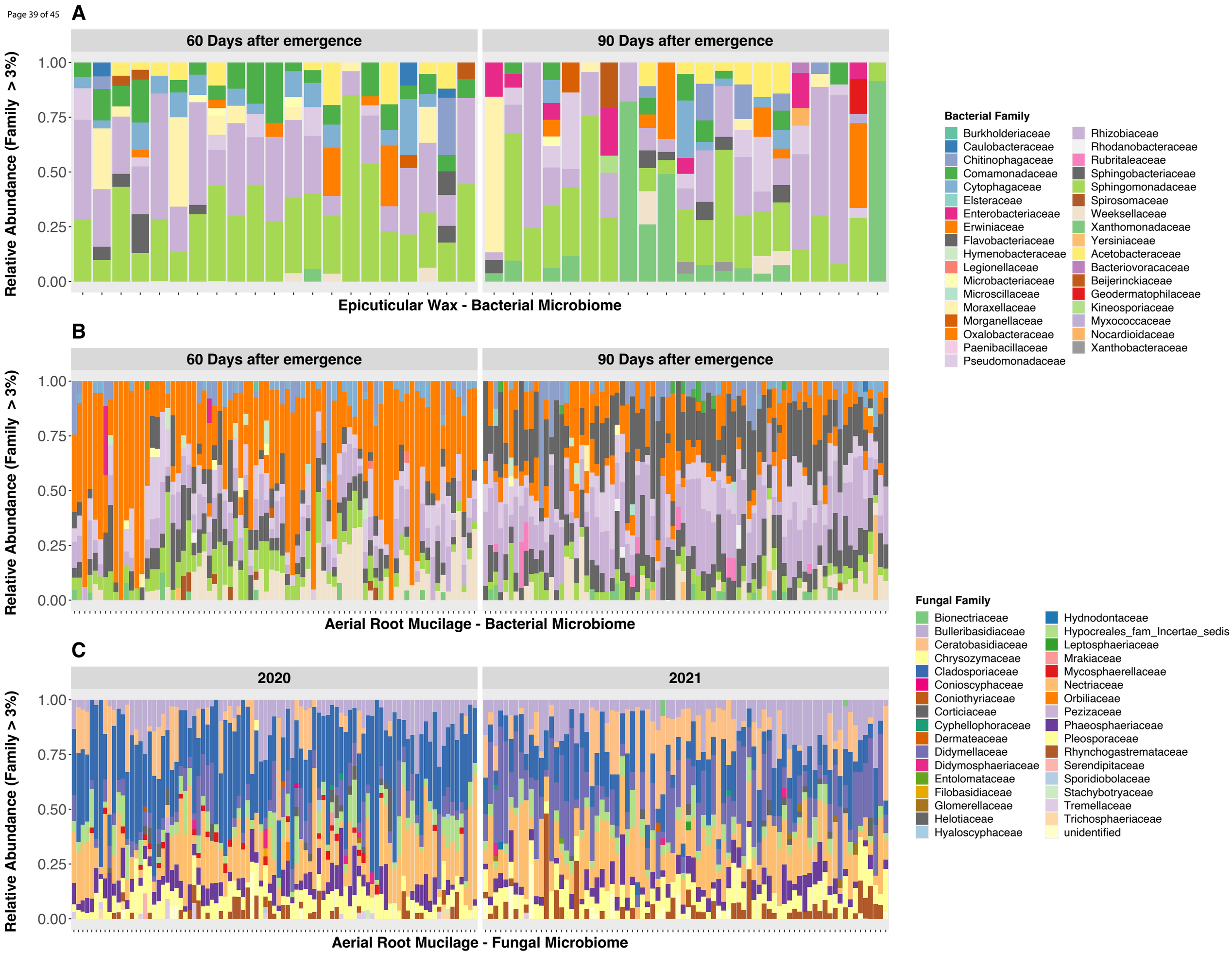
A
60 Days after emergence
90 Days after emergence
Relative Abundance (Family > 3%)
1.00
0.75
0.50
0.25
0.00
Epicuticular Wax - Bacterial Microbiome
Bacterial Family
Burkholderiaceae
Caulobacteraceae
Chitinophagaceae
Comamonadaceae
Cytophagaceae
Elsteraceae
Enterobacteriaceae
Erwiniaceae
Flavobacteriaceae
Hymenobacteraceae
Legionellaceae
Microbacteriaceae
Microscillaceae
Moraxellaceae
Morganellaceae
Oxalobacteraceae
Paenibacillaceae
Pseudomonadaceae
Rhizobiaceae
Rhodanobacteraceae
Rubritaleaceae
Sphingobacteriaceae
Sphingomonadaceae
Spirosomaceae
Weeksellaceae
Xanthomonadaceae
Yersiniaceae
Acetobacteraceae
Bacteriovoracaceae
Beijerinckiaceae
Geodermatophilaceae
Kineosporiaceae
Myxococcaceae
Nocardioidaceae
Xanthobacteraceae
B
60 Days after emergence
90 Days after emergence
Relative Abundance (Family > 3%)
1.00
0.75
0.50
0.25
0.00
Aerial Root Mucilage - Bacterial Microbiome
C
2020
2021
Relative Abundance (Family > 3%)
1.00
0.75
0.50
0.25
0.00
Aerial Root Mucilage - Fungal Microbiome
Fungal Family
Bionectriaceae
Bulleribasidiaceae
Ceratobasidiaceae
Chrysozymaceae
Cladosporiaceae
Conioscyphaceae
Coniothyriaceae
Corticiaceae
Cyphellophoraceae
Dermateaceae
Didymellaceae
Didymosphaeriaceae
Entolomataceae
Filobasidiaceae
Glomerellaceae
Helotiaceae
Hyaloscyphaceae
Hydnodontaceae
Hypocreales_fam_Incertae_sedis
Leptosphaeriaceae
Mrakiaceae
Mycosphaerellaceae
Nectriaceae
Orbiliaceae
Pezizaceae
Phaeosphaeriaceae
Pleosporaceae
Rhynchogastremataceae
Serendipitaceae
Sporidiobolaceae
Stachybotryaceae
Tremellaceae
Trichosphaeriaceae
unidentified

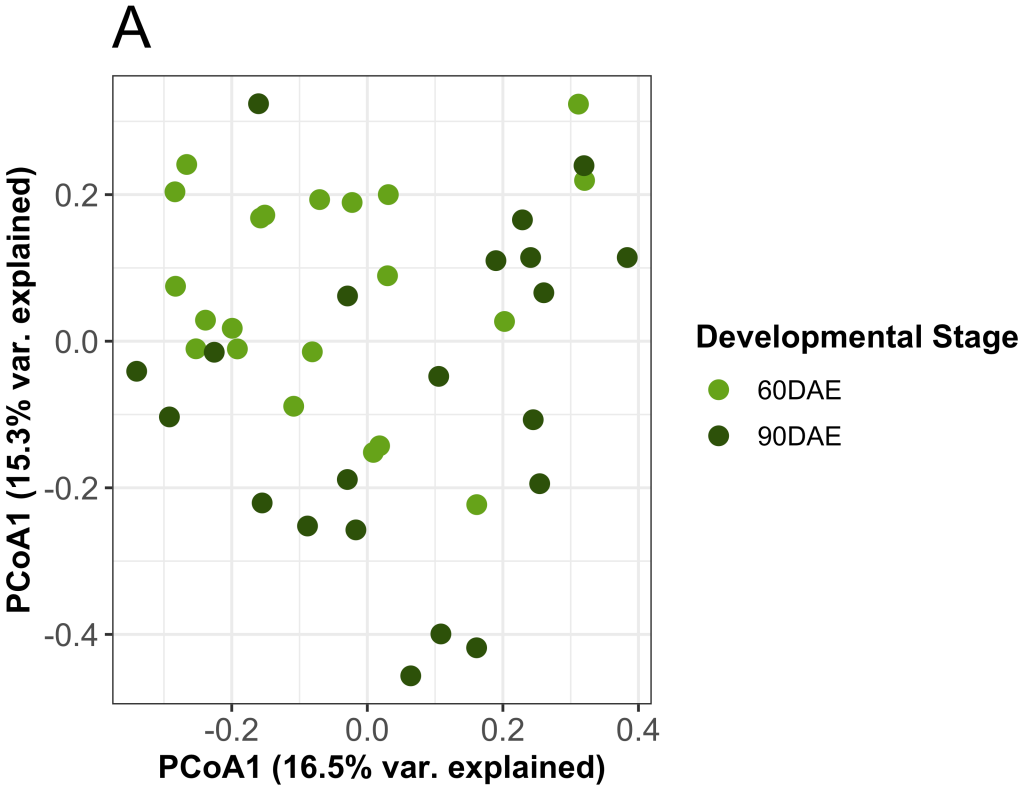
A
PCoA1 (15.3% var. explained)
PCoA1 (16.5% var. explained)
0.2
0.0
-0.2
-0.4
-0.2
0.0
0.2
0.4
Developmental Stage
60DAE
90DAE

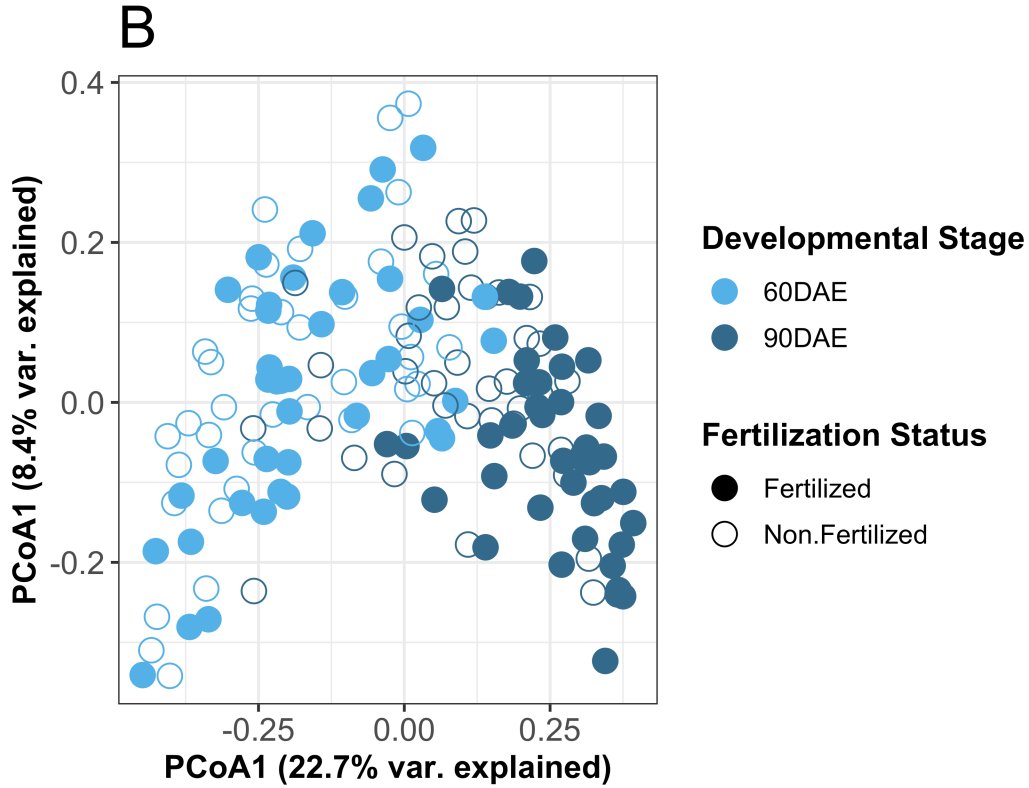
B
PCoA1 (8.4% var. explained)
PCoA1 (22.7% var. explained)
0.4
0.2
0.0
-0.2
-0.25
0.00
0.25
Developmental Stage
60DAE
90DAE
Fertilization Status
Fertilized
Non.Fertilized

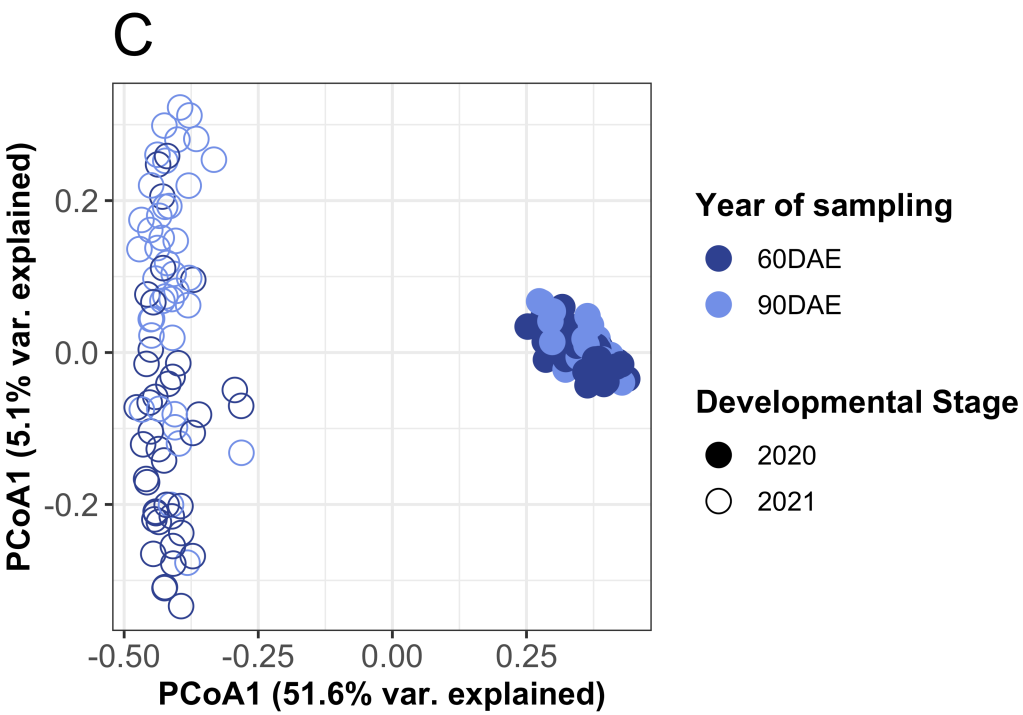
C
PCoA1 (5.1% var. explained)
PCoA1 (51.6% var. explained)
0.2
0.0
-0.2
-0.50
-0.25
0.00
0.25
Year of sampling
60DAE
90DAE
Developmental Stage
2020
2021

Mucilage microbiome
Differentially abundant ASVs: 60 vs 90 DAE

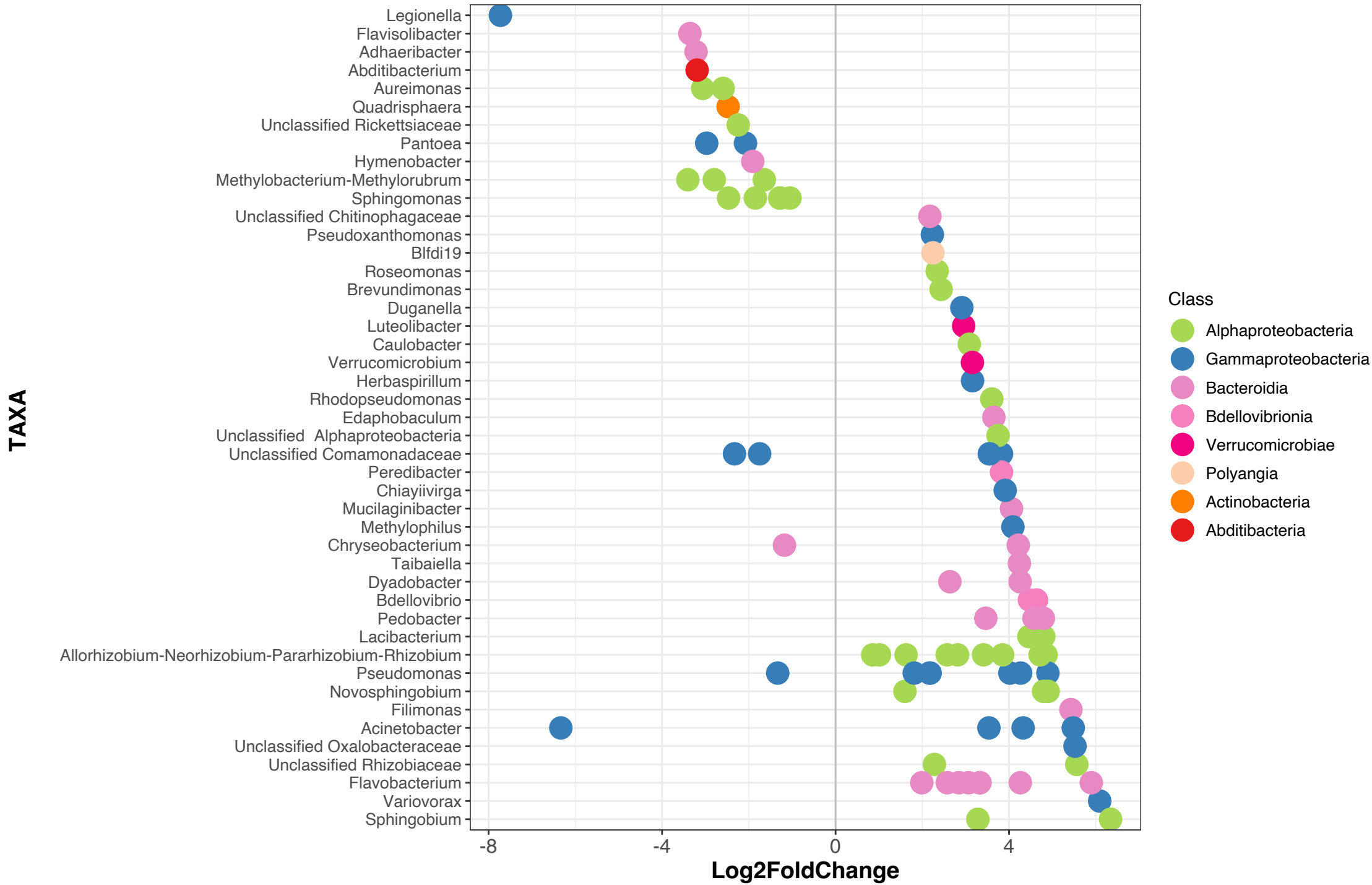

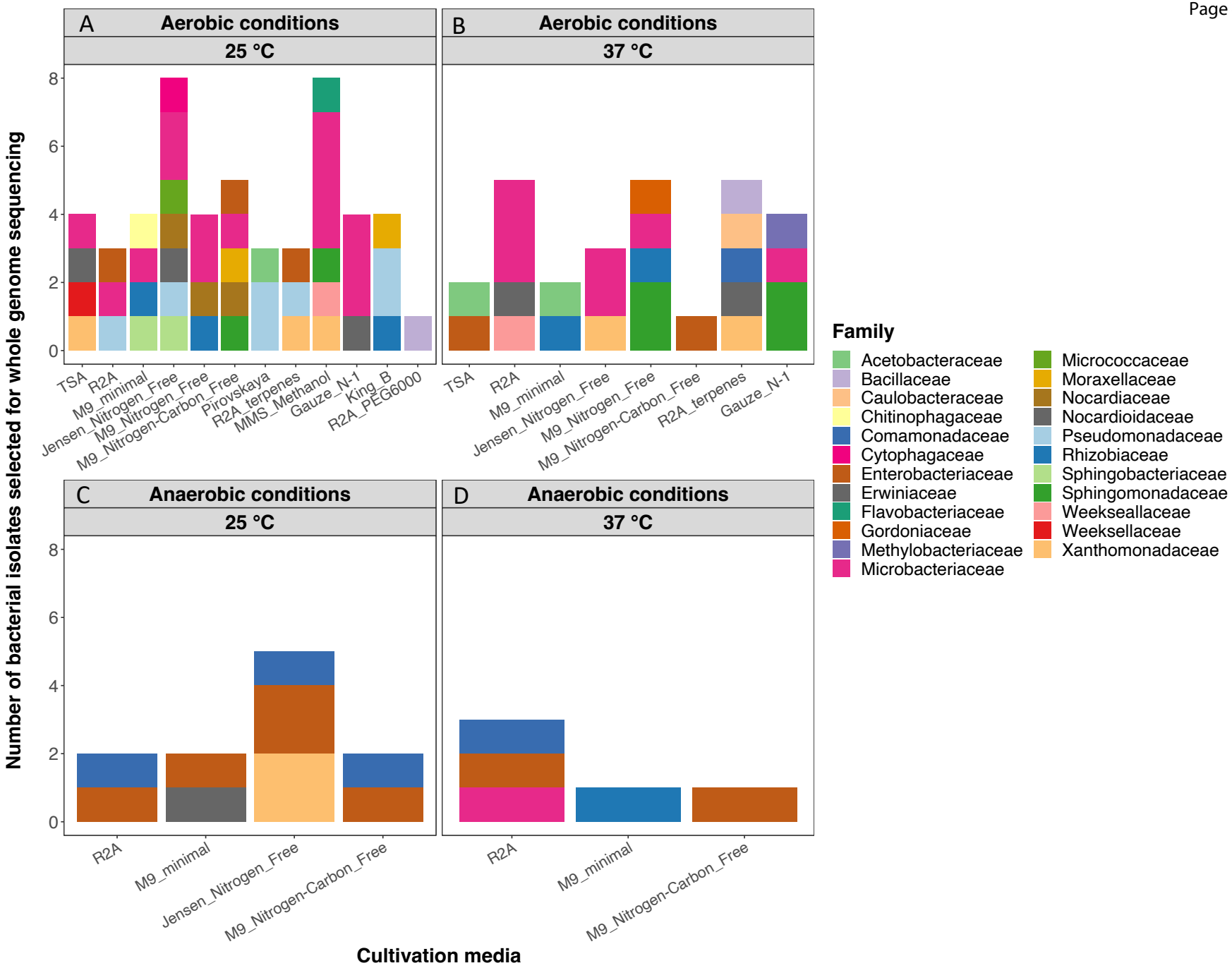
A
Aerobic conditions
25 °C
B
Aerobic conditions
37 °C
C
Anaerobic conditions
25 °C
D
Anaerobic conditions
37 °C
Number of bacterial isolates selected for whole genome sequencing
0
2
4
6
8
TSA
R2A
M9_minimal
Jensen_Nitrogen_Free
M9_Nitrogen_Free
M9_Nitrogen-Carbon_Free
Pirovskaya
R2A_terpenes
MMS_Methanol
Gauze_N-1
King_B
R2A_PEG6000
Cultivation media
Family
Acetobacteraceae
Bacillaceae
Caulobacteraceae
Chitinophagaceae
Comamonadaceae
Cytophagaceae
Enterobacteriaceae
Erwiniaceae
Flavobacteriaceae
Gordoniaceae
Methylobacteriaceae
Microbacteriaceae
Micrococcaceae
Moraxellaceae
Nocardiaceae
Nocardioidaceae
Pseudomonadaceae
Rhizobiaceae
Sphingobacteriaceae
Sphingomonadaceae
Weekseallaceae
Weeksellaceae
Xanthomonadaceae

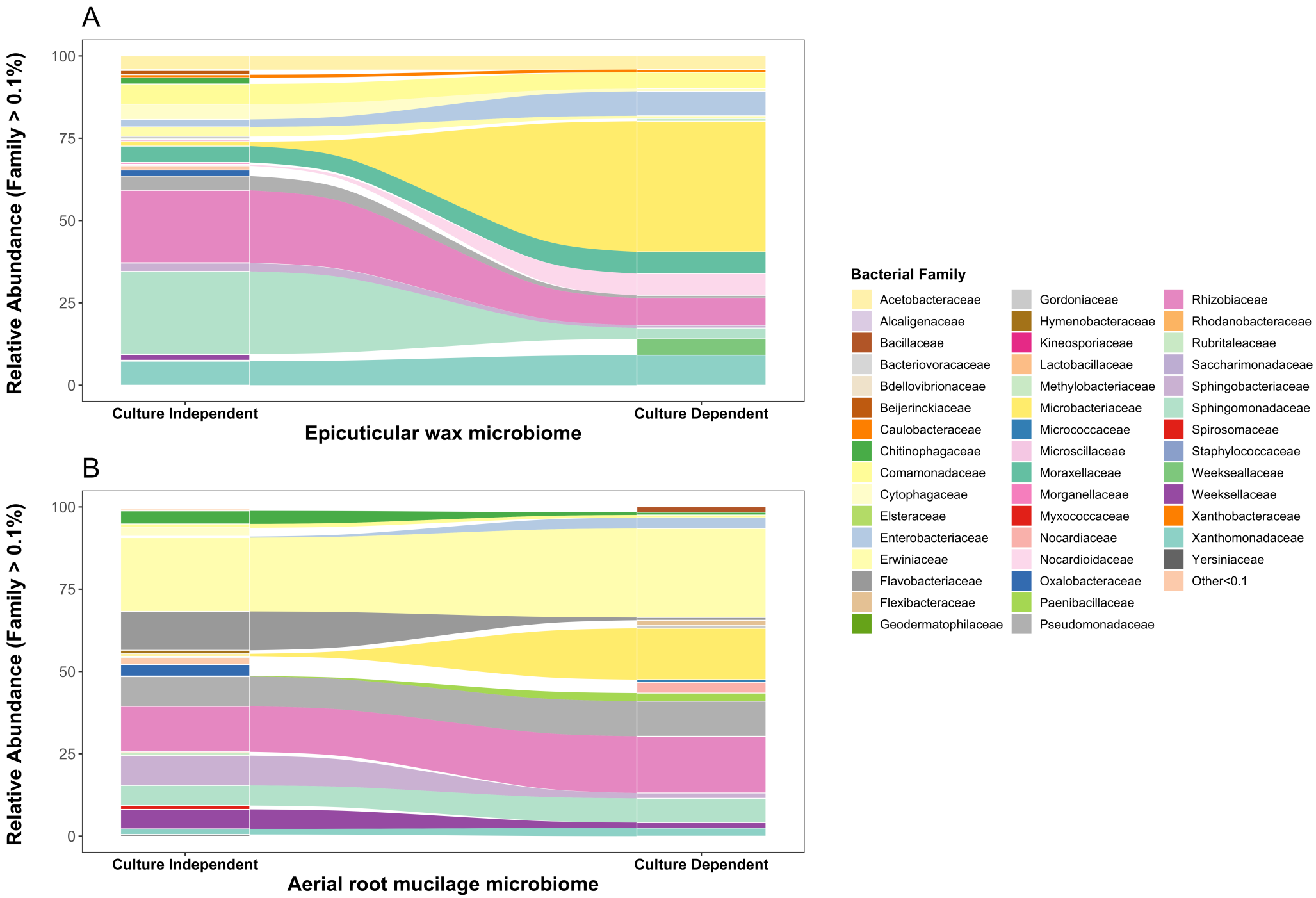
A
Relative Abundance (Family > 0.1%)
100
75
50
25
0
Culture Independent
Culture Dependent
Epicuticular wax microbiome
B
Relative Abundance (Family > 0.1%)
100
75
50
25
0
Culture Independent
Culture Dependent
Aerial root mucilage microbiome
Bacterial Family
Acetobacteraceae
Alcaligenaceae
Bacillaceae
Bacteriovoracaceae
Bdellovibrionaceae
Beijerinckiaceae
Caulobacteraceae
Chitinophagaceae
Comamonadaceae
Cytophagaceae
Elsteraceae
Enterobacteriaceae
Erwiniaceae
Flavobacteriaceae
Flexibacteraceae
Geodermatophilaceae
Gordoniaceae
Hymenobacteraceae
Kineosporiaceae
Lactobacillaceae
Methylobacteriaceae
Microbacteriaceae
Micrococcaceae
Microscillaceae
Moraxellaceae
Morganellaceae
Myxococcaceae
Nocardiaceae
Nocardioidaceae
Oxalobacteraceae
Paenibacillaceae
Pseudomonadaceae
Rhizobiaceae
Rhodanobacteraceae
Rubritaleaceae
Saccharimonadaceae
Sphingobacteriaceae
Sphingomonadaceae
Spirosomaceae
Staphylococcaceae
Weekseallaceae
Weeksellaceae
Xanthobacteraceae
Xanthomonadaceae
Yersiniaceae
Other<0.1

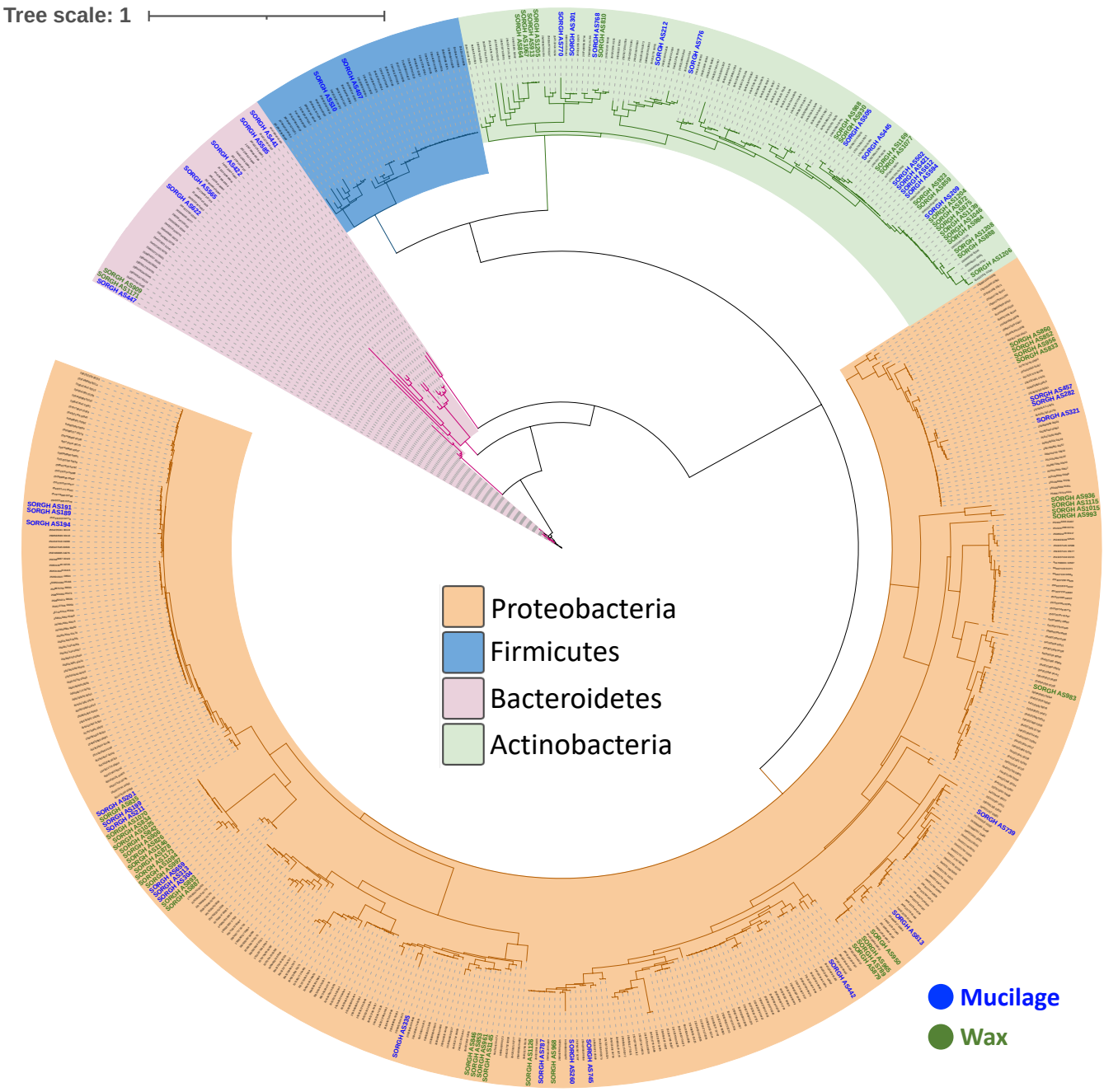
Tree scale: 1
Proteobacteria
Firmicutes
Bacteroidetes
Actinobacteria
Mucilage
Wax

A

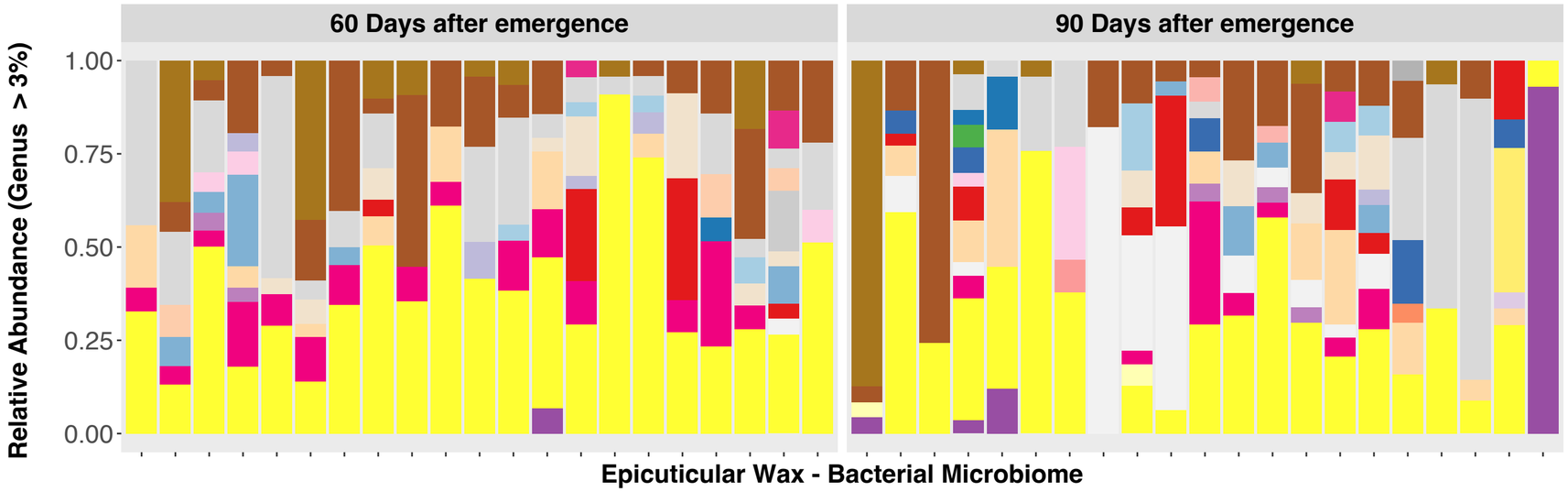

B

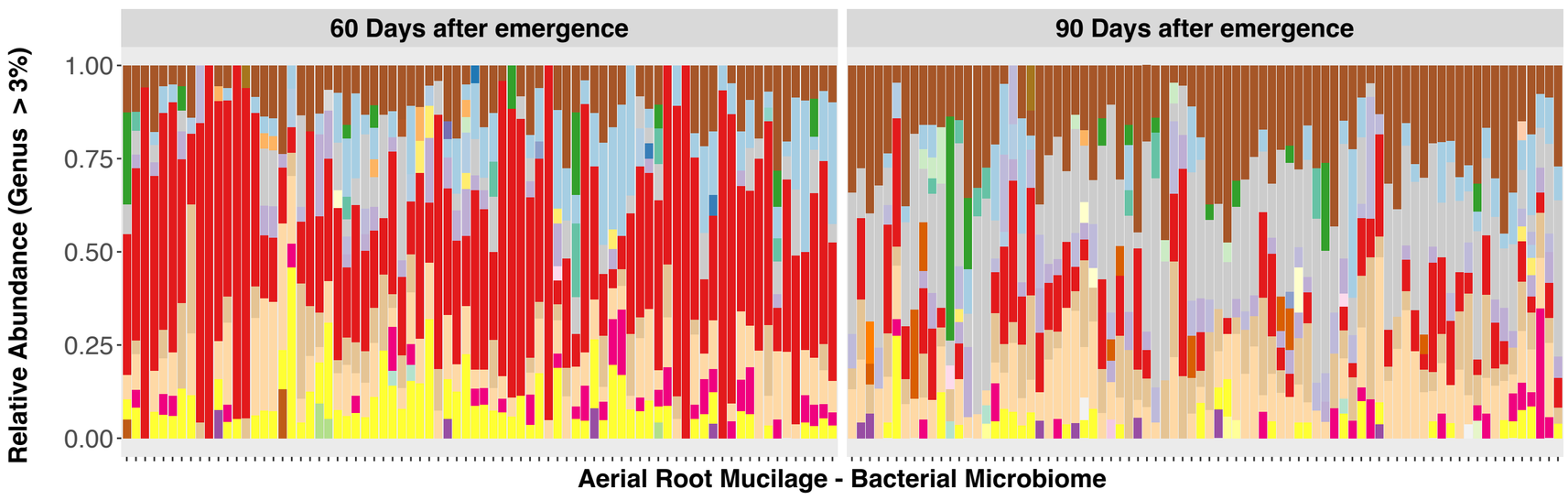

C

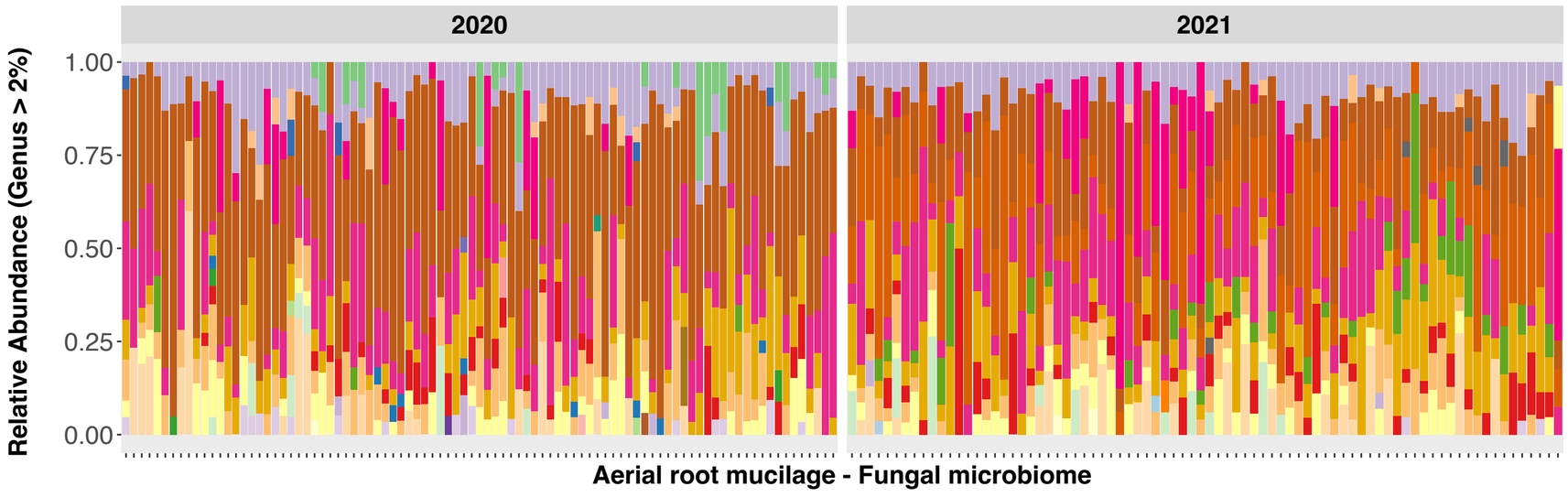

Bacterial Genus

- Acinetobacter
- Allorhizobium-Neorhizobium-Pararhizobium-Rhizobium
- Aureimonas
- Brevundimonas
- Buchnera
- Burkholderia-Caballeronia-Paraburkholderia
- Chitinophaga
- Chryseobacterium
- Curtobacterium
- Duganella
- Dyadobacter
- Filimonas
- Flavobacterium
- Flexibacter
- Herbaspirillum
- Hymenobacter
- Lacibacterium
- Legionella
- Luteibacter
- Luteolibacter
- Massilia
- Mucilaginibacter
- Novosphingobium
- Paenibacillus
- Pantoea
- Pedobacter
- Pseudomonas
- Pseudoxanthomonas
- Siphonobacter
- Sphingobium
- Sphingomonas
- Spirosoma
- Stenotrophomonas
- Taibaiella
- uncultured
- Variovorax
- Xanthomonas
- Aeromicrobium
- Ancylobacter
- Asaia
- Blastococcus
- Cytophaga
- Escherichia-Shigella
- Granulibacter
- Methylobacterium-Methylorubrum
- Nubsella
- P3OB-42
- Peredibacter
- Quadrisphaera
- Roseomonas
- Sphingobacterium

Fungal Genus

- Acremonium
- Alternaria
- Articulospora
- Bipolaris
- Bulleromyces
- Ceratobasidium
- Cladosporium
- Colletotrichum
- Cyphellophora
- Epicoccum
- Filobasidium
- Fusarium
- Gibberella
- Hannaella
- Laetisaria
- Leptosphaeria
- Mollisia
- Mycosphaerella
- Neosetophoma
- Nigrospora
- Orbilia
- Papiliotrema
- Phaeosphaeria
- Protocreopsis
- Pseudopithomyces
- Sampaiozyma
- Sarocladium
- Stachybotrys
- Tausonia
- Trechispora
- unidentified
- Vishniacozyma
- Waitea
- Wojnowicia